Modelling the impact of proportion, sowing date, and architectural traits of a companion crop on foliar fungal pathogens of wheat in crop mixtures

Sébastien Levionnois[1,2*], Christophe Pradal[3,4], Christian Fournier[5], Jonathan Sanner[1], Corinne Robert[1]

[1]UMR EcoSys, INRAE, AgroParisTech, Campus Agro Paris-Saclay, 91120 Palaiseau, France
[2]UMR AGAP Institut, Univ. Montpellier, CIRAD, INRAE, Institut Agro, 34398 Montpellier, France
[3]CIRAD, UMR AGAP Institut, 34398 Montpellier, France.
[4]Inria & LIRMM, Univ. Montpellier, CNRS, 34090 Montpellier, France
[5]UMR LEPSE, Université de Montpellier, INRAE, Montpellier SupAgro, 34000 Montpellier, France

*Corresponding author: S. Levionnois; e-mail: sebastien.levionnois.pro@gmail.com

Funding: This work was funded by the Horizon 2020 framework program (reference: IPM Decisions 817617).

Author contributions

S.L. and C.R. designed the study; all authors designed the model; S.L. and J.S. developed the model; S.L. and C.R. analyzed the model; S.L. wrote the manuscript with contributions from C.R. and C.P.

ABSTRACT

Diversification of cropping systems is a lever for the management of epidemics**.** However, most research to date has focused on cultivar mixtures, especially for cereals, even though crop mixtures can also improve disease management. To investigate the benefits of crop mixtures, we studied the effect of different crop mixture characteristics (i.e., companion proportion, sowing date, and traits) on the protective effect of the mixture. We developed a SEIR (Susceptible, Exposed, Infectious, Removed) model of two damaging wheat diseases (*Zymoseptoria tritici* and *Puccinia triticina*), which were applied to different canopy components, ascribable to wheat and a theoretical companion crop. We used the model to study the sensitivity of disease intensity to the following parameters: wheat-vs.-companion proportion, companion sowing date and growth, and architectural traits. For both pathogens, the companion proportion had the strongest effect, with 25% of companion reducing disease severity by 50%. However, changing companion growth and architectural traits also significantly improved the protective effect. The effect of companion characteristics was consistent across different weather conditions. After decomposing the dilution and barrier effects, the model suggested that the barrier effect is maximized for an intermediate proportion of companion crop. Our study thus supports crop mixtures as a promising strategy to improve disease management. Future studies should identify real species and determine the combination of host and companion traits to maximize the protective effect of the mixture.

Keywords: Septoria tritici blotch, wheat leaf rust, intercropping, crop mixture, biological regulation, fungal epidemic

INTRODUCTION

Disease management in intensive cropping systems faces numerous challenges: agrosystem vulnerability to disease outbreaks is set to increase with climate change and global biodiversity loss (Větrovský *et al.*, 2019; Carmona *et al.*, 2020), pesticide use comes at high economic, human health and environmental cost (Bourguet & Guillemaud, 2016), and pathogens often adapt to resistant cultivars and pesticides (Brown, 2015; Hawkins *et al.*, 2019). Diversification of cropping systems appears to be an important lever to improve the durability of disease management (Malézieux *et al.*, 2009; Ratnadass *et al.*, 2012; Beillouin *et al.*, 2021). Previous studies on cereal-based mixtures in the field level mainly focused on cultivar mixtures (Wolfe, 1985; Finckh *et al.*, 2000; Mundt, 2002). Disease reduction in cultivar mixtures is based on two important mechanisms (Burdon & Chilvers, 1982; Wolfe, 1985; Finckh *et al.*, 2000): the dilution and barrier effects. The dilution effect occurs when the proportion of the susceptible component decreases, then diminishing the resource available for the pathogen. The barrier effect occurs when resistant plants intercept spores on their trajectory, then preventing them from reaching susceptible plants. Other mechanisms are pathogen competition, induced resistance or disruptive selection (Borg *et al.*, 2018; Clin *et al.*, 2021).

Three main drivers related to agricultural practices may impact the efficacy of the dilution and density effects and finally the overall protective effect of the mixture. The first driver is the genetic composition of the mixture, determined by (i) the relative proportion of resistant vs. susceptible components, (ii) the difference in the resistance level against the targeted disease between resistant and susceptible components, and (iii) the number of resistant cultivars. Most studies on cultivar mixtures for disease management have focused on these characteristics (see references in Finck *et al.*, 2000; Mundt, 2002; Huang *et al.*, 2012; Borg *et al.*, 2018), showing that increasing both the resistant proportion and the level of host resistance against the targeted pathogen increases the protective effect across different crops. This includes cereals and wheat for both airborne (e.g., rust) and rain-borne (e.g., septoria) dispersal diseases (Huang *et al.*, 2012; Borg *et al.*, 2018; M'Barek *et al.*, 2020; Kristoffersen *et al.*, 2020).

A second driver is the spatial distribution of resistant plants and organs (i.e., leaves and stems) in the field, which is determined by plant architecture and planting arrangement. Regarding plant architecture, traits such as plant height and leaf area index (LAI; $m^2\ m^{-2}$) can impact disease severity (Calonnec *et al.*, 2013; Vidal *et al.*, 2017a) by improving the escape of the host plant from the spores, or spore interception by the companion barrier plant. Regarding the barrier effect, this was shown for rain-borne diseases such as Septoria tritici blotch (Vidal *et al.*, 2017b, 2018), although this is potentially true for airborne diseases such as rust (Frezal

et al., 2009). Planting arrangement has mainly been investigated through genotype unit area (GUA), i.e., the ground area occupied by an independent, continuous, and homogenous unit of host genotype (Mundt & Browning, 1985). Most of studies support that decreasing GUA improves the mixture effect on disease reduction (Mundt & Browning, 1985; Mundt & Leonard, 1986; Brophy & Mundt, 1991; Newton & Guy, 2009; Gigot *et al.*, 2014).

A third driver that may impact the protective effect of the mixture is the temporal distribution of resistant plants and organs in the field, which is determined by the sowing date or potentially by different phenological and plant growth dynamics between the susceptible and resistant components. The objective here is to synchronize the presence of resistant host tissue with the pathogen development and release (e.g., maximizing the barrier effect against spore dispersal), and to desynchronize the presence of susceptible host tissue with the pathogen (Calonnec *et al.*, 2013; Robert *et al.*, 2018). However, this driver is difficult to be explored in cultivar mixtures, as the desynchronization of cultivars is not desired.

The findings to date are mainly based on cultivar mixtures, whereas investigations on crop mixtures for the biological control of fungal diseases in annual crops are critically lacking. We argue that cereal-based crop mixtures can be beneficial for cereal disease management for several reasons. (1) Across cultivars of a given crop, disease resistance is often quantitative, and the pathogen can adapt through evolution, meaning that the resistance of a so-called 'resistant' host is never definitive and complete (de Vallavieille-Pope *et al.*, 2012; Rimbaud *et al.*, 2021). However, as pathogens are usually specific to crop species, a different crop (e.g., legumes) would be qualitatively and definitively resistant to the cereal pathogen, thus enhancing the protective effect and its durability against diseases. (2) Plant architecture and phenology are generally more contrasted between crop species than between cultivars of a given crop species (Gaudio *et al.*, 2019; Evers *et al.*, 2019). This can be an opportunity to maximize the barrier effect against spore dispersal and to optimize the synchronicity between epidemics and the barrier. (3) Crop mixtures can add other ecosystem services such as resource use efficiency, quantity and quality yields, soil conservation, and biological regulation of pests and weeds (Beillouin *et al.*, 2021).

These three mixture drivers (i.e., genetic composition, spatial and temporal distributions) have rarely been investigated simultaneously in a single study. Several models have been developed for cultivar mixtures to quantify (i) the effect of the susceptible-vs.-resistant proportion (Jeger *et al.*, 1981; Sapoukhina *et al.*, 2013; Gigot *et al.*, 2014; Mikaberidze *et al.*, 2015), (ii) the effect of plant architecture (Vidal *et al.*, 2018), or (iii) the effect of GUA (Goleniewski & Newton, 1994; Gigot *et al.*, 2014). However, to our knowledge, no modelling

framework provides the opportunity to incorporate several drivers. Such a modelling framework would allow to hierarchize the main mixture characteristics in terms of its protective effect and to examine the optimal trade-offs between protective effect and yield. Moreover, although the dilution and barrier effects are frequently referred to in studies investigating cultivar mixtures for disease management (e.g., Borg *et al.*, 2018; Vidal *et al.*, 2018), these effects and their relative contributions to the reduction of disease severity are rarely quantified (Burdon & Chilvers, 1982; Chin & Wolfe, 1984). This quantification would allow to optimize the mixture design by maximizing the barrier effect while minimizing the dilution effect, which would in turn maximize both the yield and protective effects.

In this study, we developed a modelling framework based on a SEIR (Susceptible, Exposed, Infectious, Removed) model applied to different canopy components: wheat and a theoretical companion crop. The model simulates a single- or mixture-crop canopy, with parameters describing the wheat-vs.-companion proportion, crop growth dynamics, crop architecture, and sowing date. The SEIR epidemic function was parameterized for two wheat fungal diseases: Septoria tritici blotch (*Zymoseptoria tritici*; STB), a rain-borne disease, and wheat leaf rust (*Puccinia triticina*; WLR), an airborne disease. We then studied the disease response to the variations in the companion characteristics. We specifically addressed the following questions: (1) To what extent can crop mixtures be used for the biological regulation of two contrasting wheat fungal pathogens? (2) What are the effects and the hierarchy of different mixture characteristics (i.e., proportion, spatial and temporal distribution) regarding the overall protective effect? Are these effects consistent across different weather scenarios? And finally, (3) what is the relative contribution of the dilution and Barrier effects in the reduction of diseases in wheat-based crop mixtures?

MODEL DESCRIPTION

The model aims to investigate how the addition of a non-host crop species to a wheat canopy can limit two wheat fungal epidemics: WLR and STB. The model analyzes the impact of the following on the epidemic dynamics: (i) the wheat:companion proportion ($P_{W:C}$), (ii) companion sowing date, and (iii) companion traits relating to architecture, growth, and phenology. We study two contrasting wheat diseases (WLR and STB) to determine how they respond to these different crop mixture characteristics.

We developed a framework based on a SEIR-like model (Li & Muldowney, 1995) describing canopy growth and epidemic dynamics during a single crop season (Fig. 1). A canopy is modelled using simple growth functions that represent only one crop or otherwise

two crops in a within-row mixture. The difference between crop species is first defined by disease susceptibility: a crop susceptible to diseases is defined as wheat, whereas the resistant companion crop that is qualitatively and definitely resistant to diseases. There is no explicit spatial structure within the canopy, although a set of parameters for each crop describes their relative proportion, growth, phenology, sowing date and canopy porosity. Direct interactions between plants (e.g., competition and facilitation) and plant resource dynamics are not taken into account. The following epidemic processes are modelled: tissue infection, latent period after infection, sporulation of infectious tissues, and the flow of spores from production to dispersal that subsequently infects the wheat.

Time is measured in degree-days (dd) and denoted by t. Time is regarded as discrete, indexed by time intervals t of 10 dd (degree-day) with an experiment duration T (dd). A cropping season starts at t_{start} with the sowing date and ends at t_{end} with the harvesting date. T is the length of the experiment such that T/t_{end} corresponds to the number of cropping seasons in the experiment. The intercropping season is modelled as an instantaneous projection from t_{end} to the start of the next cropping season; in other words, the time between the end of the current cropping season and the start of the next cropping season is not explicitly simulated. However, during this time interval, some state variables are projected onto the start of the next cropping season with appropriate modifications. For instance, a fraction of spores survives and is remobilized in the next cropping season (see below). Our model is formalized as a discrete-time analogue of a continuous-time logistic model.

All abbreviations of the model parameters and state variables are given in Tables 1 and 2.

The model is implemented in Python 3 and available as open source software on Github (https://zenodo.org/record/7139051#.Y_N1FB-ZPIV; Sanner *et al.*, 2022). The main outputs can be reproduced with Jupyter notebook tutorials.

Healthy crop within-row *mixtures*

The crop canopy is quantified in crop *LAI* (leaf area index; $m^2\ m^{-2}$). At each time step t, for each crop j, and in the absence of disease in the system, $LAIj_{,t}$ is decomposed in two states according to the *SEIR* model: the susceptible surface S ($m^2\ m^{-2}$) and the removed surface R ($m^2\ m^{-2}$):

$$LAI_{j,t} = S_{j,t} + R_{j,t}$$

The growth dynamics of crop $S_{j,t}$ are described by a growth function. $S_{j,t}$ grows from t = 0 to $t = t_{onto,J}$, where $t_{onto,j}$ (dd) is the senescence earliness for crop j. Leaf senescence of crop j occurs at a constant rate μ_j. The theoretical canopy growth $S_{j,t}^{th}$ with no disease is given as:

$$S_{j,t+1}^{th} = S_{j,t}^{th} + c_t - \mu_j S_{j,t}^{th}$$

with a logistic growth function:

$$c_t = \begin{cases} \beta_j S_{j,t}^{th}\left(1 - \frac{S_{j,t}^{th}}{K_j}\right) if\ t \leq t_{onto} \\ 0\ otherwise \end{cases}$$

where β_j is the intrinsic growth rate for crop j and K_j(m² m^{-2}) the carrying capacity attributed to crop j. At t = 0, c_0 is initialized with $S_{j,0} = K_j/1000$. The model user must be aware that the discrete-time analogue of the continuous-time logistic equation can generate negative recruitment. Therefore, the following conditions must be respected: $0 < S_{j,0} < K_j$ and $\beta_j < 0$.

For a healthy canopy, the dynamics of senescent tissues are described as:

$$R_{j,t+1} = R_{j,t} + \mu_j S_{j,t}^{th}$$

Eventually, the whole canopy will die once it has completed its life cycle, at the end of the cropping season. R then equals LAI.

Finally, for a mixture of J crops, the total $LAI_{tot,t}$ is given by:

$$LAI_{tot,t} = \sum_{j=1}^{J} S_{j,t} + \sum_{j=1}^{J} R_{j,t}$$

The carrying capacity K remains unchanged in the case of a pure stand or a mixture. In the case of a mixture, the different crops share the carrying capacity (K) in variable proportions depending on the mixture under investigation. The share of K is given by:

$$K = \sum_{j=1}^{J} K_j$$

SEIR function in within-row crop mixtures

In the event of disease in the system, the LAI of the susceptible crop, LAI_W, is decomposed into four states according to the *SEIR* model: susceptible surface S_W, exposed (i.e., infected but latent) surface E_W, infectious surface I_W, and senescent and removed surface R_W (all expressed in m² m^{-2}):

$$LAI_{W,t} = S_{W,t} + E_{W,t} + I_{W,t} + R_{W,t}$$

At date t_{inf}, the start date of the epidemic, S_W becomes exposed to the disease. Then, at each time, a quantity S_{W_inf} of susceptible tissues becomes infected (from S_W to I_W), and a quantity $\Delta_{E \to I}$ of exposed tissues becomes infectious (from E_W to I_W). S_{W_inf} and $\Delta_{E \to I}$ are determined by different infection, spore production, and spore dispersal state variables and parameters described in detail below. For STB, the dynamics of I_W also depend on the emptying

of pycnids at a rate ψ with rain events such that the emptying of a given I_W surface leads to I_W death. Then the higher ψ, the faster infectious tissues will release spores and die thereafter, which finally decreases the spore source. Susceptible and exposed tissues S_W and E_W become senescent after t_{onto}, while infected tissues (I_W) immediately become senescent at a rate μ_W in all cases. Then, the general *SEIR* function is described as:

$$S_{W,t+1} = S_{W,t} + c_t - S_{W\_inf,t} - \mu_W.S_{W,t}.1_{t \geq t_{onto}}$$

$$E_{W,t+1} = E_{W,t} + S_{W\_inf,t} - \Delta_{E \to I,t} - \mu_W.E_{W,t}.1_{t \geq t_{onto}}$$

$$I_{W,t+1} = \begin{cases} I_{W,t} + \Delta_{E \to I,t} - \psi.I_{W,t}.rain_t - \mu_W.I_{W,t} & for\ septoria \\ I_{W,t} + \Delta_{E \to I,t} - \mu_W.I_{W,t} & for\ rust \end{cases}$$

$$R_{W,t+1} = \begin{cases} R_{W,t} + \mu_W(S_{W,t} + E_{W,t}).1_{t \geq t_{onto}} + \mu_W.I_{W,t} + \psi.I_{W,t}.rain_t & for\ septoria \\ R_{W,t} + \mu_W(S_{W,t} + E_{W,t}).1_{t \geq t_{onto}} + \mu_W.I_{W,t} & for\ rust \end{cases}$$

where $rain_t$ is a Boolean with the value 1 to express a rain event at t.

Spore interception and infection of susceptible tissues

For spore interception by the canopy, we assume two processes analogous to light interception and absorbance. In the first process, spores intercepted by the canopy are partitioned between the wheat and companion crop according to a dominance factor based on the ERIN (evaporation and radiation interception of neighboring plants) model (Wallace, 1997). Reflecting the extent to which a plant or canopy covers another, the dominance factor then partially integrates the height difference. Depending on the dominance factor, the canopy extinction coefficient is partitioned between the two canopies such that a higher and denser canopy will have a higher coefficient. The rationale is that taller plants have a theoretically greater chance of being on the trajectory of a given spore than their smaller counterparts. In the second process, despite the lack of empirical evidence, we assume that spore interception by the canopy is analogous to light interception, thus following a Beer-Lambert law (Barillot *et al.*, 2011).

The spore fraction intercepted by wheat for the two extreme conditions in which wheat is dominant ($f_{D,W}$) or is completely dominated under the canopy ($f_{U,W}$) are calculated as:

$$f_{D,W,t} = 1 - e^{-b_W.(S_{W,t} + E_{W,t} + I_{W,t})}$$

$$f_{U,W,t} = e^{-b_C * S_{C,t}}.(1 - e^{-b_W.(S_{W,t} + E_{W,t} + I_{W,t})})$$

with b_W and b_C being spore interception coefficients for wheat and the companion crop, respectively, such that the greater the b coefficient, the larger the fraction of intercepted spores. We assume that S_W, E_W and I_W for wheat and S_C for companion are the surfaces that intercept spores. Then, the total spore fraction intercepted by wheat F_W depending on its dominance factor D_W is given by:

$$F_{W,t} = f_{U,W,t} + D_W.(f_{D,W,t} - f_{U,W,t})$$

with D_W as the wheat dominance factor calculated as:

$$D_W = \frac{h_W}{h_W + h_C}$$

with h_W and h_C as a proxy for the height of the wheat and companion crop respectively. The fraction intercepted by the companion crop F_C depending on its dominance factor D_C is calculated in the same way as Fw, such that:

$$f_{D,C,t} = 1 - e^{-b_C.S_{C,t}}$$

$$f_{U,C,t} = e^{-b_W.(S_{W,t} + E_{W,t} + I_{W,t})}.(1 - e^{-b_C.S_{C,t}})$$

$$F_{C,t} = f_{U,C,t} + D_C.(f_{D,C,t} + f_{U,C,t})$$

$$D_{C,t} = 1 - D_W = \frac{h_C}{h_W + h_C}$$

with $f_{D,C}$ and $f_{U,C}$ as the spore fraction intercepted by the companion for the two extreme conditions in which the companion is the most dominant and the most dominated plant, respectively. Then, ε_t is the spore fraction intercepted by the entire canopy:

$$\varepsilon_t = F_{W,t} + F_{C,t}$$

The number of spores $N_{g,t}$ intercepted by wheat, which germinate and lead to lesions on the wheat, is given by:

$$N_{g,t} = F_{W,t}.\pi_{inf}.N_{sp,t}$$

with π_{inf} as an infection probability factor and N_{sp} the total number of spores dispersed (formation explained below). We assume that these spores spread randomly as follows: the intercepting canopy fraction is divided into elementary surfaces s_0 that represent the constant lesion size. Then, $(S_W+E_W+I_W)/s_0$ determines the maximal number of infectious spores that can be intercepted. Following a Poisson law, each elementary surface intercepts only one infectious spore from $N_{g,t}$, which then becomes a lesion. The canopy fraction F_{cont} intercepting the spores that lead to lesions is given by:

$$F_{cont,t} = 1 - exp\,(-\frac{N_{g,t}}{(S_{W,t} + E_{W,t} + I_{W,t})/s_0})$$

Assuming that spores spread over S_W, E_W, and I_W, the quantity of susceptible tissue becoming infected $S_{W\_inf}(t)$ at time t is given by:

$$S_{W\_int,t} = F_{cont,t}.S_{W,t}$$

Latent period

The transition from E_W to I_W, the latent period, is described by an age-structured vector η_t that represents at t the amount of latent tissues (or lesions) for each lesion age u, while taking into account their development since their date of appearance. This was of particular interest given the substantial difference in the latent period (Précigout *et al.*, 2020a) between WLR (around 100 dd) and STB (around 200 dd).

$$\eta_t = \begin{pmatrix} \eta_{t,1} \\ \eta_{t,2} \\ \dots \\ \eta_{t,\lambda+\delta_{EI}} \end{pmatrix}$$

The age of latent tissues u increases from 1 to $\lambda+\delta_{EI}$ such that λ is the fixed latent period and δ_{EI} is a parameter that takes into account the variability of the latent period. This method avoids having infected tissues (E_W) that rapidly begin to sporulate if the transition rate from E_W to I_W is constant in time.

The transition from E_W to I_W is impossible when the lesion age is in [1; λ - δ_{EI}[and progressive when it is in [λ - δ_{EI} ; λ + δ_{EI}], with the fraction g_u increasing to 1 when u increases toward λ + δ_{EI}. Then, for each time t, a fraction g_u of η with an age u moves to the I_W state with g_u given by:

$$g_u = \begin{cases} 0 \; \forall \; u \in [1; \lambda - \delta_{EI}[\\ \frac{1}{2 * \delta_{EI} + 1} * (u - (\lambda - \delta_{EI} - 1)) \forall \; u \in [\lambda - \delta_{EI}; \lambda + \delta_{EI}[\\ 1 \; \forall \; u = \lambda + \delta_{EI} \end{cases}$$

Then, the transition from E_W to I_W at time t is given by:

$$\Delta_{E \to I,t} = \sum_{u=1}^{\lambda + \delta_{EI}} g_u \eta_{t,u}$$

The vector η is modified according to the following relations:

$$\eta_{t+1,1} = S_{W\_int,t}$$

$$\eta_{t+1,u} = (1 - \mu_W)\eta_{t,u-1}(1 - g_{u-1}) \; if \; u \in [2, \lambda + \delta_{EI}]$$

Spore dynamics

The dispersal process is different between STB and WLR. For STB, dispersal occurs through rain-borne pycnidiospores and airborne ascospores. Pycnidiospores, which are splash-dispersed during rain events, represent most of the spores produced and primarily drive the epidemic during the cropping season. Ascospores are dispersed by wind, potentially across long distances (Morais *et al.*, 2015). For WLR, dispersal only occurs through airborne urediospores.

For both diseases, three spore sources potentially trigger and/or supply the epidemic: (i) soil, (ii) spore clouds from outside the canopy, and (iii) spores produced within the canopy during epidemics. For both diseases, the model initialization is set with an initial soil inoculum Sp_{init} and a spore cloud coming from the outside of the canopy (Table 1). The main driver for the start of the epidemic is the initial soil inoculum for STB and spore clouds for WLR. For STB, the initial soil inoculum is composed of either pycnidiospores or ascospores (Suffert & Sache, 2011; Morais *et al.*, 2015).

First, there may be spores in the soil or alternative local hosts, represented by the spore soil reservoir P. At the beginning of the season, a quantity $Sp_{soil,t}$ from P_t can contribute to the canopy infection. For STB, which is a rain-borne disease, we assume that the initial inoculum mostly comes from soil and that this soil-based infection occurs in autumn when the leaves are close to the ground at the beginning of the growth phase. From date t_{out}, we assume that the leaves are out of reach of the spores (Garin *et al.*, 2014). Furthermore, leaf infection occurs only during rain events. For WLR, which is an airborne disease, the disease starts later in the cropping season during spring after date t_{inf} when the infection begins (Garin *et al.*, 2014). Then, $Sp_{soil,t}$ is described as follows:

$$Sp_{soil,t} = \begin{cases} \max\left(0, \left(1 - \frac{t}{t_{out}}\right) P_t\right) rain_t & for\ septoria \\ P_t 1_{t \geq t_{inf}} & for\ rust \end{cases}$$

where $rain_t$ is a Boolean taking the value 1 when expressing a rain event in time t.

Second, the canopy can also be initially infected or affected by a spore cloud $Sp_{ext,t}$ from outside the canopy throughout the cropping season. $Sp_{ext,t}$ mainly changes according to a fixed parameter, Sp_{ext}. At each time step, the fraction of $Sp_{ext,t}$ that is not retained by the canopy falls onto the soil and supplies P_t, before supplying $Sp_{soil,t}$ as described above. This external spore cloud is parameterized for a given period (for 200 dd after growth start t_{start}) and for a given interval (every 20 dd), corresponding to the daily and regular dispersal of spores by wind.

Third, once the epidemic has started, the most important source is spore production by sporulant tissues Sp_{canopy}. A spore fraction will also disperse "outside" the canopy, although we assume that this fraction will be taken into account in the spore fraction produced and dispersed from "outside" and coming into the canopy. Therefore, the overall spore production is assumed to remain in the canopy in the current model. As rain-borne spores, pycnidiospores (STB) are dispersed during rain events. As airborne spores, ascospores (STB) and urediospores (WLR) are dispersed at daily intervals (every 20 dd). Thus, $Sp_{canopy,t}$ is given as follows:

$$Sp_{canopy,s,t} = \begin{cases} \sigma_s I_t rain_t \ \ for\ rain-borne\ spores \\ \sigma_s I_t\ every\ 20dd\ for\ air-borne\ spores \end{cases}$$

with σ_s as the spore production rate for each type of spore s.

These three inoculum sources constitute the total number of spores $N_{sp,t}$ dispersed and potentially intercepted by and infecting the canopy at time t:

$$N_{sp,t} = Sp_{soil,t} + Sp_{ext,t} + Sp_{canopy,t}$$

The pool P is supplied by the spore fraction $1 - \varepsilon_t$ from $N_{sp,t}$, which is not intercepted by the canopy, and by the spore fraction $(1 - \pi_{inf}).\varepsilon_t$ from $N_{sp,t}$, which is intercepted by the canopy but does not germinate and supplies Sp_{soil} as described above. The dynamics of spore P_t are given by:

$$P_{t+1} = P_t + (1 - \varepsilon_t)N_{sp,t} + (1 - \pi_{inf})\varepsilon_t N_{sp,t} - \rho P_t - Sp_{soil,t}$$

The different terms of the equation of P_{t+1} successively represent: (i) spores not intercepted by crops and falling to the soil, (ii) spores intercepted by crops but not germinating and infecting and then falling to the soil or being leached, (iii) spore mortality, and (iv) spore fraction from the pool P that is re-dispersed. For the transition from one cropping season to another, we assume that the reproductive structures that still contain spores empty any remaining spores into the pool P at the end of the cropping season. Then, we assume that a spore fraction θ of the pool P survives into the intercropping season:

$$P_{t_{end}+1} = \theta(P_{t_{end}} + \sigma_s I_{W,t_{end}})$$

Quantification of disease intensity

To quantify the disease intensity, we first quantified the cumulated canopy sporulating surface I_{vid}, which is the cumulated canopy surface that has already passed through the infectious state I, such that:

$$I_{vid,t} = \sum_{i=0}^{t} \Delta_{E \to I}$$

Based on I_{vid}, the *AUDPC* (area under disease progress curve) is a more integrated quantification of disease intensity, which takes into account both the earliness and severity of the disease (Précigout *et al.*, 2017). *AUDPC* is calculated as the integral of the infectious surface *I.* In our case, it is simply a sum given that we use a discrete time:

$$AUDPC_t = \sum_{i=0}^{t} I_{vid}$$

To keep comparability across experiments with different companion proportion, we standardized all *AUDPC* values by the maximum *AUDPC* with a scenario of pure wheat (such as $K_W = K = 6$) for a given disease and a given weather scenario (in the case of STB) by calculating a relative *AUDPC*:

$$relative\ AUDPC = \frac{AUDPC}{AUDPC_{K_{max}}}$$

Then, this relative *AUDPC* varies between 0 and 1 such that the higher the relative *AUDPC*, the lower the protective effect of the mixture and the closer it is to pure wheat.

MODEL ANALYSIS

Parameterization and initialization

Wheat growth and phenological parameters were determined by fitting and calibrating the logistic growth model on previously published data (Dornbusch *et al.*, 2011; Baccar, 2011). The experimental design and calibration method are presented in Supplemental Method S1 and the data are available in Supplemental Material. The same parameters were fixed for the companion crop as a reference. For the disease, most of the parameters were chosen (in terms of their order of magnitude) from the literature for WLR and STB (Robert *et al.*, 2004b, 2005; Pariaud *et al.*, 2009; Frezal *et al.*, 2009; Baccar *et al.*, 2011; Garin *et al.*, 2014, 2018; Précigout *et al.*, 2020b). Some epidemic parameters that are difficult to measure were unknown and thus estimated from consistency tests (σ, π_{inf}, ρ, θ $Sp_{,ext}$, Sp_{init}). Specifically, these parameters were chosen so that the maximum disease severity I_{vid} at the end of the cropping season for wheat monoculture did not exceed three-quarters of the *LAI* for STB and two-thirds of the *LAI* for WLR in favorable weather conditions (Bancal *et al.*, 2007). The sensitivity of disease severity *Ivid* to these parameters (Fig. S1) was tested in a biologically plausible range of confidence (-10% and +10%). All parameters along with their associated literature references or specified consistency tests are presented in Table 1.

As a criteria, the interannual variation in SEIR state variables for pure wheat should be nearly null for a given weather scenario in order to mimic equilibrium (i.e., roughly equivalent outputs for successive cropping seasons). Epidemics were initialized for different values of the initial inoculum into the soil ($P_{t=0}$) for WLR and STB as well as for Sp_{ext} (Table 1). An example of the epidemic dynamics over three cropping seasons for both diseases in pure wheat and with 50% of companion crop is illustrated in Fig. 2. The model was developed using Python.

Simulations

Each simulation corresponds to one cropping season, with the initial conditions reproducing equilibrium across several cropping seasons for pure wheat. To test the robustness of the effect of the companion characteristics on epidemics, we tested different weather conditions. For STB, rainfall data (but not temperature) were used for the dispersal of pycnidiospores, based on daily-monitored at the meteorological station of INRA-Grignon (78850 France). To analyze the effect of rainfall on STB dynamics, we used the year 1997 as the reference for the average rainfall year, 2000 as the high rainfall year, and 1995 as the low rainfall year. For WLR, we used the date of the onset of epidemics (t_{inf}) to simulate the favorable, average, and unfavorable conditions (800, 1000, and 1200 dd respectively; Garin *et al.*, 2018).

Local sensitivity analyses for all parameters

To first frame the overall behavior of the model and the sensitivity to wheat-vs.-companion-vs.-pathogen traits, we conducted local sensitivity analysis for each model parameter p (Table 1). We investigated how small changes in size Δp in the value of this parameter affect the mixture infection rate for the different spatial arrangements. We calculated the relative sensitivity $e(p)$ of the infection rate to parameter p as Berghuijs *et al.* (2020):

$$e(p) = \frac{p}{Y(p)}\frac{dY(p)}{dp} = \frac{p}{Y(p)} . \frac{Y(p + \Delta p) - Y(p - \Delta p)}{2.\Delta p}$$

with $Y(p)$ as the infection rate for a given value of parameter p and $\Delta p = 0.1p$.

Sensitivity of disease intensity to mixture characteristics

To analyze the sensitivity of disease intensity and the protective effect of the mixture to wheat-vs.-companion proportions $P_{W:C}$ and parameters relating to the companion sowing dates and the companion architectural and growth traits, we used two approaches. First, to analyze the continual response of disease intensity to $P_{W:C}$, we changed the proportion of the companion crop in the mixture by including the full range of $P_{W:C}$ divided into 50 steps ranging from pure companion to pure wheat. We conducted this analysis individually for each parameter and also by varying the parameters between -50% and 50% from the reference, as this variation was assumed to be comparable to interspecific differences (Table 1; Fig. S2). For the sowing date, these variation rates were calculated relative to the cropping season length.

Second, to analyze the continual response of the disease intensity to parameters relating to the companion sowing dates and companion architectural and growth traits, we analyzed the sensitivity of disease intensity by comparing seven different values of each parameter

individually: -50%, -40%, -20%, reference, 20%, 40%, and 50%. We also applied this analysis to five different proportions of wheat within the mixture: 10%, 30%, 50%, 70%, and 90%.

Regarding the companion crop characteristics, two traits are related to plant architecture: h_C and b_C. They respectively change the dominance level (a proxy of height) and canopy absorbance (a proxy of leaf density and leaf angle), and then the spore interception capacity of the canopy. β_C, μ_C, and $t_{onto,C}$ were the growth curve parameters of the companion crop (Fig. S2). The higher the β_C, the sooner the companion crop will reach a large *LAI*. The higher the μ_C, the faster *LAI* will be lost after $t_{onto,C}$. The higher the $t_{onto,C}$, the longer the period will be with a large or maximum green *LAI*.

Dilution-vs.-barrier decomposition

To quantify the dilution-vs.-barrier effect and its contribution to the overall protective effect, we compared different scenarios of two component mixtures with different wheat-vs.-companion proportions $P_{W:C}$. We first ran 50 experiments with the pure wheat stand evenly distributed in the range of K_W from 0 to 5 m^2 m^{-2}. Then, we considered the variation of *I* along this range as the dilution effect alone. Second, we ran 60 experiments of mixtures with the same total carrying capacity *K* of 6 m^2 m^{-2}, which we assumed to be the mean wheat *LAI* in monoculture (Benbi, 1994). The carrying capacity of the wheat and companion crop K_W and K_C, respectively vary such that:

$$K = K_W + K_C = 6 \text{ m}^2 \text{ m}^{-2}$$

For the 60 experiments of mixtures, K_W ranged from 0 to 6 m^2 m^{-2} and then varied in relative proportions from 0 to 1 with K_C. Then, we considered the variation of *I* along this range, as the addition of both the dilution and barrier effect.

Based on these two sets of 60 experiments, we decomposed the barrier effect from the dilution effect for different wheat-vs.-companion proportions $P_{W:C}$. First, for the pure susceptible stand, we calculated the protective effect of dilution $E_{dilution}$ as the percent reduction in *AUDPC* distributed in the range of K_W from 0 to 6 m^2 m^{-2} relative to the maximum *AUDPC* ($K = 6$ m^2 m^{-2}):

$$E_{dilution} = \left(\frac{AUDPC_{pure,K=6} - AUDPC_{pure,K_W}}{AUDPC_{pure,K=6}} \right)$$

Then, for the mixture, we calculated the total protective effect of the mixture E_{total} as the percent reduction in *AUDPC* distributed in the range of K_W from 0 to 6 m^2 m^{-2} relative to the maximum *AUDPC* found in pure wheat:

$$E_{total} = \left(\frac{AUDPC_{pure,K=6} - AUDPC_{mixture,K_W}}{AUDPC_{pure,K=6}} \right)$$

Then, we calculated the protective effect of the companion crop as a barrier $E_{barrier}$, as follows:

$$E_{barrier} = E_{tot} - E_{dilution}$$

RESULTS

Overall effects of parameters

Based on local sensitivity analyses for all parameters (wheat, companion, and pathogen traits), for the top ten parameters, disease intensity expressed as relative *AUDPC* was most sensitive to wheat ($t_{,onto,W}$, $P_{W:C}$, β_W, μ_W, h_W) and pathogens traits (t_{inf}, π_{inf}, λ, σ_U, ρ) for WLR and to wheat (β_W, $P_{W:C}$, b_W, h_W), companion ($delta_C$, β_C, h_C) and pathogen traits (π_{inf}, σ_P, ψ) for STB (Fig. 3). Sensitivity to companion traits was the weakest from the top ten parameters (β_C and h_C for STB). Relative *AUDPC* was consistently sensitive to five out the top ten parameters for both diseases (π_{inf}, $P_{W:C}$, σ, β_W, h_W; Fig. 3).

Effect of proportions

For both diseases, there was a general trend with a continual non-linear decrease in relative *AUDPC* when increasing the proportion of the companion crop in the mixture (Fig. 4; Fig. 5; Fig. S3; Fig. S4). However, there was a difference in the effect level between both diseases, as the protective effect of the mixture was slightly higher (lower disease intensity) for STB compared to WLR for a given $P_{W:C}$. For WLR, relative *AUDPC* was reduced by ~50% with 25% of companion proportion, and by ~75% with 50% of companion proportion (Fig. 4). For STB, the effect was slightly stronger, and relative *AUDPC* was reduced by ~60% with 25% of companion proportion, and by ~80% with 50% of companion proportion (Fig. S3).

For both diseases, favorable conditions largely increased the disease intensity (Fig. S5; Fig. S6; Fig. S7). However, favorable, average, and unfavorable weather conditions did not differently influence the shape of the *AUDPC* response to $P_{W:C}$ (Fig. S5).

Effect of sowing date and companion traits

Regarding the sowing date ($delta_C$) and the five tested companion traits (h_C, b_C, β_C, μ_C, $t_{onto,C}$), most had a substantial effect on relative *AUDPC* for both diseases (Fig. 4; Fig. 5; Fig. S3; Fig. S4). Four types of response were identified. (1) We found a linear response of relative *AUDPC* with h_C and b_C, as increasing the dominance factor and the interception coefficient decreased the disease intensity (Fig. 5a,b; Fig. S4a,b). (2) We observed threshold effects for β_C and $t_{onto,C}$,

as decreasing the growth rate and advancing the start of senescence in relation to the reference increased the disease intensity, although increasing these parameters from the reference had mostly no effect on disease intensity (Fig. 5c,e; Fig. S4c,e). (3) The response of relative *AUDPC* to $delta_C$ was different for the two diseases due to the different degrees of synchronicity for the wheat and companion dynamics and the different dates of infection (start of the growing season for STB vs. 800 dd for WRL). For WRL, both delaying and advancing sowing date in relation to the reference increased disease intensity (Fig. 5f). For STB, we found a threshold effect, as advancing the sowing date from the reference had no effect, while delaying this parameter from the reference increased disease intensity (Fig. S4f). (4) For both diseases, the mortality rate μ_C had almost no effect (Fig. 5d; Fig. S4d).

The effect on relative *AUDPC* was dependent on the parameter considered in terms of the sowing date and companion traits. The strongest effects were found for β_C and $delta_C$. For instance, decreasing the growth rate by 50% led to an increase of ~20% in disease intensity for both diseases (for 50% of wheat in the mixture; Fig. 5c; Fig. S4c). Furthermore, delaying the sowing date by 50% led to an increase of ~20-25% in disease intensity depending on the disease (for 50% of wheat in the mixture; Fig. 5f; Fig. S4f). Average effects were found for h_C and b_C, with ~10-15% variation in relative *AUDPC* when decreasing these parameters by 50% (Fig. 5a,b; Fig. S4a,b). For t_{onto}, a rather strong effect was found for WRL, although it was average for STB (Fig. 5e; Fig. S4e).

For both diseases, the effect of a given companion trait or sowing date on relative *AUDPC* was dependent on the companion proportion, with a null effect for pure wheat or pure companion, and a maximum effect generally with a 25-50% of companion proportion (Fig. 4; Fig. S3). Overall, for both diseases, there was no interaction between weather conditions and trait variations, as there was no difference in the shape of *AUDPC* response to trait variations for favorable, average, and unfavorable weather conditions (Fig. S6; Fig. S7). For some traits, for both diseases, the response to trait variations was slightly stronger for a 50% companion proportion and for favorable weather conditions: h_C, b_C, β_C, and $delta_C$.

Decomposition of dilution and barrier effects

When decomposing the overall protective effect of the mixture with regard to the dilution and barrier effects across the range of wheat-companion proportions $P_{W:C}$, we found consistent patterns for both diseases (Fig. 6). The dilution effect was monotonic and always increased with higher companion proportions, although this increase was non-linear as it accelerated toward higher companion proportions. The barrier effect was non-monotonic, first increasing from 0

to 60% of companion proportion for WLR and from 0 to 45% for STB before decreasing. The overall protective effect was mostly linear.

DISCUSSION

Here, we present an innovative model of a crop within-row mixture to investigate the impact of fungal epidemics on wheat. The model supports crop mixtures as a promising method for the biological regulation of foliar fungal epidemics. It provides some ideas about the companion characteristics that optimize the protective effect of the mixture, regardless of the weather conditions. The proportion of the companion crop in the mixture strongly impacts disease intensity through a combination of dilution and barrier effects.The sowing date and companion architectural traits can also impact disease intensity. The limitations and perspectives of the model and crop mixtures for epidemic regulation are discussed.

Overall sensitivity of epidemics to model parameters

Regarding the overall sensitivity of epidemics in the model, the parameters related to wheat architectural and growth traits (h_W, b_W, β_W, $t_{onto,W}$) are the strongest determinants. This is in agreement with the fact that epidemics are first sensitive to resource availability (described here by green LAI), as the wheat growth rate and start of senescence determine the duration of green LAI during the crop season (Calonnec *et al.*, 2013). This finding is also in line with several experimental (Burdon & Chilvers, 1982; Mundt *et al.*, 2011) and modelling studies (Robert *et al.*, 2008, 2018; Papaïx *et al.*, 2014; Garin *et al.*, 2018), which demonstrate that resource availability through green LAI dynamics is a primary driver of epidemics at various spatial scales (canopy, field, landscape levels). However, resource availability is determined not only by leaf surface but also by "leaf quality" through carbon and nitrogen content (Robert *et al.*, 2005; Lecompte *et al.*, 2013, 2017; Précigout *et al.*, 2017). This feature is not modelled here, although it could be reflected by the effect of spore production rates (σ_U and σ_P) in our model, as leaf nitrogen content drives the spore production rate (Robert *et al.*, 2002).

Epidemics are also sensitive to resource accessibility, i.e., the capacity of spores to reach new healthy leaves as wheat grows during the season (Robert *et al.*, 2008, 2018; Calonnec *et al.*, 2013; Garin *et al.*, 2018). Relating to wheat traits, this feature is approximated in our model by the wheat dominance factor and Beer-Lambert coefficient, which reflect the wheat height and canopy porosity to spores, respectively, and integrate of several putative traits that drive interception such as plant height, LAI, leaf area density (LAD; $m^2\ m^{-3}$), and leaf angle (Madden

& Boudreau, 1997; Ando *et al.*, 2007; Schoeny *et al.*, 2008; Arraiano *et al.*, 2009; Calonnec *et al.*, 2013; Vidal *et al.*, 2018).

Some epidemic parameters were also strong determinants (t_{inf}, π_{inf}, λ, σU and σP, ψ, ρ). These parameters are directly related to the efficacy of spore production and dispersal (σU and σP, ψ) as well as infection (π_{inf} and λ), which are key parameters in the pathogen aggressiveness and overall epidemics (Pariaud *et al.*, 2009; Suffert *et al.*, 2013).

Impact of wheat-based crop mixtures

The wheat:companion proportion ($P_{W:C}$) was the strongest driver controlling disease intensity. Higher companion proportions were associated with a higher protective effect, in agreement with several meta-analyses demonstrating that increasing the non-host proportion in wheat and cereal cultivar mixtures decreases disease intensity (Finckh *et al.*, 2000; Huang *et al.*, 2012; M'Barek *et al.*, 2020). For both diseases, introducing a ~25% companion proportion reduced disease intensity by 50%, which is in agreement with the study of M'Barek *et al.* (2020) on STB. Therefore, crop mixtures are a promising practice for the biological regulation of fungal epidemics. Crop mixtures with a different crop can provide a total and definitive resistance against some specific diseases, whereas cultivars used for biological regulation generally have resistance that can be overcome on evolutionary timescales (de Vallavieille-Pope *et al.*, 2012; Rimbaud *et al.*, 2021). Moreover, crop mixtures can add other ecosystem services as discussed below.

In terms of the processes, increasing the companion proportion increases not only the dilution effect but also the barrier effect. Disentangling the dilution and barrier effects explains the non-linear relationship between *AUDPC* and $P_{W:C}$ for both diseases, as illustrated in Fig.6. First, as the dilution and barrier effects are both non-linear, their addition results in the *AUDPC* curve. Second, the non-linear relationship between the dilution effect and the wheat proportion mainly reflects the Beer-Lambert law underlying spore interception, which is exponential as low LAI values disproportionately intercept more spores, while larger values are close to the asymptote. Third, the non-linear relationship between the barrier effect and the wheat proportion reflects the fact that the barrier effect is insignificant for low LAI values of wheat (stronger dilution effect) as well as for high LAI values of wheat (companion LAI too low to have a barrier effect). Then, we demonstrated that according to $P_{W:C}$, the barrier effect displays threshold effects, with a maximal barrier effect around a 60% proportion of companion crop for WLR and 50% for STB. To our knowledge, two studies have decomposed the dilution and barrier effects. (Burdon & Chilvers, 1977) showed that (i) the barrier effect arises beyond 50%

of companion crop and that (ii) the dilution effect is linear, which is inconsistent with our results. Chin & Wolfe (1984) showed that at a proportion of 17% wheat and 83% companion crop, the overall protective effect can reach ~80% with the equal contribution of dilution and barrier effects, which is consistent with our results. This finding calls for further quantification of dilution-vs.-barrier effects.

Identifying these thresholds allows to investigate the optimal $P_{W:C}$ that maximizes the barrier effect in comparison to the dilution effect: for instance, increasing the companion proportion beyond a certain threshold (here, 60%) has a low marginal protective effects This paves the way for maximizing the protective effect while not diminishing the crop and yield of interest. The optimal barrier effect will also change with the sowing date and companion architectural traits (discussed below) as well as with pathogen dispersal, and phenological and aggressiveness traits. The current model might be an interesting tool for such optimizations.

Impact of sowing date and companion traits

Companion sowing date, growth rate, and start of senescence had the strongest effects on disease intensity, with a 20% variation in simulated disease intensity. The companion dominance factor and Beer-Lambert coefficient had average effects, with a 10-15% variation in disease intensity. However, only the dominance factor and Beer-Lambert coefficient reduced disease intensity compared to the reference parameters.

The companion dominance factor and Beer-Lambert coefficient reflect the companion height and canopy porosity to spores, respectively, and integrate several putative traits that drive interception such as plant height, LAI, LAD, and leaf angle (Madden & Boudreau, 1997; Ando *et al.*, 2007; Schoeny *et al.*, 2008; Arraiano *et al.*, 2009; Calonnec *et al.*, 2013; Vidal *et al.*, 2018). However, while the traits driving the dominance factor and Beer-Lambert coefficient must minimize spore interception for wheat, these traits must also maximize spore interception to maximize the barrier effect of the companion crop (Vidal *et al.*, 2017b,a, 2018). Accordingly, it was shown that beyond the absolute trait value of plant height or LAI regarding spore interception (Madden & Boudreau, 1997; Schoeny *et al.*, 2008; Arraiano *et al.*, 2009), for cultivar mixtures it is the difference in plant height and LAI between host and resistant components that drives epidemics (at least for STB: Vidal *et al.*, 2017b,a, 2018). Specifically, a shorter companion with a higher LAI, but the opposite traits for the host, maximize the barrier effect. Therefore, both the host and companion traits should be analyzed together in future experimental and modelling studies.

It is noteworthy that our results for the dominance factor, which is a proxy for plant height, are not in agreement with the findings of Vidal *et al.* (2018) regarding STB. Due to the short-distance transport of rain-borne spores through rain drops, as green leaves develop from the bottom to the top during plant development, shorter vertical distances between leaves increases the opportunities for spores to colonize (Arraiano *et al.*, 2009; Robert *et al.*, 2018). Then, a protective effect is favored in mixtures with tall host plants but small resistant plants (Vidal *et al.*, 2018). This inconsistency strongly advocates for not only considering spore interception as analogical to light interception, as the dominance factor is not sufficient to describe and take into account the effect of host and companion heights on epidemics. First, the different physical processes underlying the dispersal of airborne and Rain-borne spores can lead to different and even opposing effects of host and companion heights on the spread of disease. Second, spores are probably not as ubiquitous as light. Thus, it may be more relevant to distinguish between the short- and Long-distance dispersal of airborne spores (Zawolek & Zadoks, 1992; Sache & Zadoks, 1996; Aylor, 1999), or to model splashed droplets (Saint-Jean *et al.*, 2004; Vidal *et al.*, 2018) instead of spores. Finally, plant height is generally negatively related to LAD, which could have confounding effects on spore interception.

Companion sowing date, growth rate, and start of senescence can increase the duration of the presence of the companion crop in the model, and thus improve the synchronicity between spore dynamics and the effective barrier on spore dispersal. This is noteworthy in the context of crop mixtures, as we demonstrated that the barrier effect is the leading process in the protective effect of mixtures when the companion proportion is between 0 and 75%. In cultivar mixtures, this phenological lever is not considered, as growth and phenological synchronicity between cultivars are favored at harvest time in standardized systems (Newton *et al.*, 2009).

The lack of effect of the companion mortality rate on disease intensity indicates that the removed leaf area R is weakly sensitive to mortality rate changes in the current model (Fig. S2). Even in the event of a drastic change in the mortality rate, which becomes unrealistic, the disease intensity still remains weakly sensitive (for instance, 8% change for a -90% mortality rate compared to the reference). This is due to the calculation of $AUDPC$ as an integral of the cumulated infectious LAI. Then, the earlier the start of senescence, the stronger the impact of the mortality rate will be on disease intensity measured here as relative $AUDPC$ here. An in-depth study is required to disentangle the effect of trait interactions on disease intensity.

Another result is noteworthy: the impact of companion characteristics does not depend substantially on weather conditions for both STB and WLR. This is a key result for the robustness of companion trait effects.

Model limitations and perspectives

This model has several limitations and perspectives that improve our understanding of the functioning of crop mixtures for biological regulation and highlight the reliability of the model for agricultural applications. First, at present, model calibration and evaluation, along with the data that allow this task, are critically lacking regarding crop mixtures for epidemic regulation. The present model could provide ideas about which experiments should be prioritized, since they are generally time-consuming and expensive, require disease and LAI monitoring, and limit the number of factors that can be studied. Based on our model and previous results on cultivar mixtures, a reasonable strategy is to explore a diversity of companion crops that reflect a diversity of architectures and phenologys to maximize the barrier effect. Moreover, the companion species used in this study was an abstraction with a growth curve identical to that of wheat and only defined in terms of its qualitative and definitive resistance to diseases. Therefore, real companion species, with contrasted architectures and phenologies should be studied in order to better identify crop species that can be used in mixtures for effective epidemic regulation, as also the combination of traits underlying these crop species. Ground cover crops can also provide an opportunity to trap spores from rain-borne diseases and maximize the protective effect (Ntahimpera *et al.*, 1998).

Second, the study of different spatial field arrangements (alternate rows or stripes, chessboard, etc.) is currently lacking (Hernández-Ochoa *et al.*, 2022), as we only studied within-row mixtures here. Therefore, the model should be scaled up to the field level with an explicit spatial structure. Third, in the past decades, research on crop mixtures has largely focused on plant-plant interactions (i.e., competition, facilitation, complementarity, compensation) and their impact on resource dynamics and over-yielding (Corre-Hellou *et al.*, 2009; Louarn & Faverjon, 2018; Gaudio *et al.*, 2019; Berghuijs *et al.*, 2020; Justes *et al.*, 2021). Given that plant-plant interactions affect the canopy development and structure and that epidemics negatively impact host resources and canopy structure (Robert *et al.*, 2004b, 2005; Bancal *et al.*, 2007), host-companion-pathogen interactions and resource feedbacks should necessarily impact the overall epidemics. From this multitrophic perspective, modelling several diseases simultaneously would also be a step forward (Garin *et al.*, 2018).

ACKNOWLEDGEMENTS

We would like to thank Bruno Andrieu for sharing the data of wheat leaf area index. We thank the two reviewers and the editor for critical and valuable comments. This study was funded by the IPM Decisions project (Horizon H2020, No. 817617).

692 **LITERATURE CITED**

693 **Ando K, Grumet R, Terpstra K, Kelly J**. **2007**. Manipulation of plant architecture to enhance crop
694 disease control. *CAB Reviews: Perspectives in Agriculture, Veterinary Science, Nutrition and Natural*
695 *Resources* **2**: 1–8.

696 **Arraiano LS, Balaam N, Fenwick PM, Chapman C, Feuerhelm D, Howell P, Smith SJ, Widdowson JP,**
697 **Brown JKM**. **2009**. Contributions of disease resistance and escape to the control of septoria tritici
698 blotch of wheat. *Plant Pathology* **58**: 910–922.

699 **Aylor DE**. **1999**. Biophysical scaling and the passive dispersal of fungus spores: relationship to
700 integrated pest management strategies. *Agricultural and Forest Meteorology* **97**: 275–292.

701 **Baccar R**. **2011**. Plasticité de l'architecture du blé d'hiver modulée par la densité et la date de semis
702 et son effet sur les épidémies de Septoria tritici.

703 **Baccar R, Fournier C, Dornbusch T, Andrieu B, Gouache D, Robert C**. **2011**. Modelling the effect of
704 wheat canopy architecture as affected by sowing density on Septoria tritici epidemics using a coupled
705 epidemic–virtual plant model. *Annals of Botany* **108**: 1179–1194.

706 **Bancal M-O, Robert C, Ney B**. **2007**. Modelling wheat growth and yield losses from late epidemics of
707 foliar diseases using loss of green leaf area per layer and pre-anthesis reserves. *Annals of Botany* **100**:
708 777–789.

709 **Barillot R, Louarn G, Escobar-Gutiérrez AJ, Huynh P, Combes D**. **2011**. How good is the turbid
710 medium-based approach for accounting for light partitioning in contrasted grass–legume
711 intercropping systems? *Annals of Botany* **108**: 1013–1024.

712 **Beillouin D, Ben-Ari T, Malézieux E, Seufert V, Makowski D**. **2021**. Positive but variable effects of
713 crop diversification on biodiversity and ecosystem services. *Global Change Biology* **27**: 4697–4710.

714 **Benbi DK**. **1994**. Prediction of leaf area indices and yields of wheat. *The Journal of Agricultural*
715 *Science* **122**: 13–20.

716 **Berghuijs HNC, Wang Z, Stomph TJ, Weih M, Van der Werf W, Vico G**. **2020**. Identification of species
717 traits enhancing yield in wheat-faba bean intercropping: development and sensitivity analysis of a
718 minimalist mixture model. *Plant and Soil* **455**: 203–226.

719 **Borg J, Kiær LP, Lecarpentier C, Goldringer I, Gauffreteau A, Saint-Jean S, Barot S, Enjalbert J**. **2018**.
720 Unfolding the potential of wheat cultivar mixtures: A meta-analysis perspective and identification of
721 knowledge gaps. *Field Crops Research* **221**: 298–313.

722 **Bourguet D, Guillemaud T**. **2016**. The hidden and external costs of pesticide use. In: Lichtfouse E, ed.
723 Sustainable Agriculture Reviews. Sustainable Agriculture Reviews: Volume 19. Cham: Springer
724 International Publishing, 35–120.

725 **Brophy LS, Mundt CC**. **1991**. Influence of plant spatial patterns on disease dynamics, plant
726 competition and grain yield in genetically diverse wheat populations. *Agriculture, Ecosystems &*
727 *Environment* **35**: 1–12.

728 **Brown JKM**. **2015**. Durable resistance of crops to disease: a Darwinian perspective. *Annual Review of*
729 *Phytopathology* **53**: 513–539.

730 **Burdon JJ, Chilvers GA**. **1977**. Controlled environment experiments on epidemic rates of barley
731 mildew in different mixtures of barley and wheat. *Oecologia* **28**: 141–146.

732 **Burdon JJ, Chilvers GA**. **1982**. Host density as a factor in plant disease ecology. *Annual Review of*
733 *Phytopathology* **20**: 143–166.

734 **Calonnec A, Burie J-B, Langlais M, Guyader S, Saint-Jean S, Sache I, Tivoli B**. **2013**. Impacts of plant
735 growth and architecture on pathogen processes and their consequences for epidemic behaviour.
736 *European Journal of Plant Pathology* **135**: 479–497.

737 **Carmona CP, Guerrero I, Peco B, Morales MB, Oñate JJ, Pärt T, Tscharntke T, Liira J, Aavik T,**
738 **Emmerson M, *et al.* 2020**. Agriculture intensification reduces plant taxonomic and functional
739 diversity across European arable systems. *Functional Ecology* **34**: 1448–1460.

740 **Chin K m., Wolfe MS**. **1984**. The spread oi Erysiphe graminis f. sp. hordei in mixtures of barley
741 varieties. *Plant Pathology* **33**: 89–100.

742 **Clin P, Grognard F, Mailleret L, Val F, Andrivon D, Hamelin FM**. **2021**. Taking Advantage of Pathogen
743 Diversity and Immune Priming to Minimize Disease Prevalence in Host Mixtures: A Model.
744 *Phytopathology®* **111**: 1219–1227.

745 **Corre-Hellou G, Faure M, Launay M, Brisson N, Crozat Y**. **2009**. Adaptation of the STICS intercrop
746 model to simulate crop growth and N accumulation in pea–barley intercrops. *Field Crops Research*
747 **113**: 72–81.

748 **Dornbusch T, Baccar R, Watt J, Hillier J, Bertheloot J, Fournier C, Andrieu B**. **2011**. Plasticity of
749 winter wheat modulated by sowing date, plant population density and nitrogen fertilisation:
750 Dimensions and size of leaf blades, sheaths and internodes in relation to their position on a stem.
751 *Field Crops Research* **121**: 116–124.

752 **Duvivier M, Dedeurwaerder G, Bataille C, De Proft M, Legrève A**. **2016**. Real-time PCR quantification
753 and spatio-temporal distribution of airborne inoculum of Puccinia triticina in Belgium. *European*
754 *Journal of Plant Pathology* **145**: 405–420.

755 **Evers JB, van der Werf W, Stomph TJ, Bastiaans L, Anten NPR**. **2019**. Understanding and optimizing
756 species mixtures using functional–structural plant modelling. *Journal of Experimental Botany* **70**:
757 2381–2388.

758 **Eyal Z**. **1971**. The kinetics of pycnospore liberation in Septoria tritici. *Canadian Journal of Botany* **49**:
759 1095–1099.

760 **Finckh MR, Gacek ES, Goyeau H, Lannou C, Merz U, Mundt CC, Munk L, Nadziak J, Newton AC,**
761 **Vallavieille-Pope C de, *et al.* 2000**. Cereal variety and species mixtures in practice, with emphasis on
762 disease resistance. *Agronomie* **20**: 813–837.

763 **Frezal L, Robert C, Bancal M-O, Lannou C**. **2009**. Local dispersal of Puccinia triticina and wheat
764 canopy structure. *Phytopathology®* **99**: 1216–1224.

765 **Garin G, Fournier C, Andrieu B, Houlès V, Robert C, Pradal C**. **2014**. A modelling framework to
766 simulate foliar fungal epidemics using functional–structural plant models. *Annals of Botany* **114**: 795–
767 812.

768 **Garin G, Pradal C, Fournier C, Claessen D, Houlès V, Robert C**. **2018**. Modelling interaction dynamics
769 between two foliar pathogens in wheat: a multi-scale approach. *Annals of Botany* **121**: 927–940.

770 **Gaudio N, Escobar-Gutiérrez AJ, Casadebaig P, Evers JB, Gérard F, Louarn G, Colbach N, Munz S,**
771 **Launay M, Marrou H, *et al.* 2019**. Current knowledge and future research opportunities for modeling
772 annual crop mixtures. A review. *Agronomy for Sustainable Development* **39**: 20.

773 **Gigot C, de Vallavieille-Pope C, Huber L, Saint-Jean S**. **2014**. Using virtual 3-D plant architecture to
774 assess fungal pathogen splash dispersal in heterogeneous canopies: a case study with cultivar
775 mixtures and a non-specialized disease causal agent. *Annals of Botany* **114**: 863–876.

776 **Goleniewski G, Newton AC**. **1994**. Modelling the spread of fungal diseases using a nearest neighbour
777 approach: effect of geometrical arrangement. *Plant Pathology* **43**: 631–643.

778 **Hawkins NJ, Bass C, Dixon A, Neve P**. **2019**. The evolutionary origins of pesticide resistance.
779 *Biological Reviews* **94**: 135–155.

780 **Hernández-Ochoa IM, Gaiser T, Kersebaum K-C, Webber H, Seidel SJ, Grahmann K, Ewert F**. **2022**.
781 Model-based design of crop diversification through new field arrangements in spatially
782 heterogeneous landscapes. A review. *Agronomy for Sustainable Development* **42**: 74.

783 **Huang C, Sun Z, Wang H, Luo Y, Ma Z**. **2012**. Effects of wheat cultivar mixtures on stripe rust: A meta-
784 analysis on field trials. *Crop Protection* **33**: 52–58.

785 **Jeger MJ, Jones DG, Griffiths E**. **1981**. Disease progress of non-specialised fungal pathogens in
786 intraspecific mixed stands of cereal cultivars. II. Field experiments. *Annals of Applied Biology* **98**: 199–
787 210.

788 **Justes E, Bedoussac L, Dordas C, Frak E, Louarn G, Boudsocq S, Journet E-P, Lithourgidis A, Pankou**
789 **C, Zhang C, *et al.* 2021**. The 4C approach as a way to understand species interactions determining
790 intercropping productivity. *Frontiers of Agricultural Science and Engineering* **1**.

791 **Kristoffersen R, Jørgensen LN, Eriksen LB, Nielsen GC, Kiær LP**. **2020**. Control of Septoria tritici blotch
792 by winter wheat cultivar mixtures: Meta-analysis of 19 years of cultivar trials. *Field Crops Research*
793 **249**: 107696.

794 **Lecompte F, Abro MA, Nicot PC**. **2013**. Can plant sugars mediate the effect of nitrogen fertilization
795 on lettuce susceptibility to two necrotrophic pathogens: Botrytis cinerea and Sclerotinia
796 sclerotiorum? *Plant and Soil* **369**: 387–401.

797 **Lecompte F, Nicot PC, Ripoll J, Abro MA, Raimbault AK, Lopez-Lauri F, Bertin N**. **2017**. Reduced
798 susceptibility of tomato stem to the necrotrophic fungus Botrytis cinerea is associated with a specific
799 adjustment of fructose content in the host sugar pool. *Annals of Botany* **119**: 931–943.

800 **Li MY, Muldowney JS**. **1995**. Global stability for the SEIR model in epidemiology. *Mathematical*
801 *Biosciences* **125**: 155–164.

802 **Louarn G, Faverjon L**. **2018**. A generic individual-based model to simulate morphogenesis, C–N
803 acquisition and population dynamics in contrasting forage legumes. *Annals of Botany* **121**: 875–896.

804 **Madden LV, Boudreau MA**. **1997**. Effect of strawberry density on the spread of anthracnose caused
805 by Colletotrichum acutatum. *Phytopathology* **87**: 828–838.

Malézieux E, Crozat Y, Dupraz C, Laurans M, Makowski D, Ozier-Lafontaine H, Rapidel B, de Tourdonnet S, Valantin-Morison M. **2009**. Mixing plant species in cropping systems: concepts, tools and models. A review. *Agronomy for Sustainable Development* **29**: 43–62.

M'Barek SB, Karisto P, Abdedayem W, Laribi M, Fakhfakh M, Kouki H, Mikaberidze A, Yahyaoui A. **2020**. Improved control of septoria tritici blotch in durum wheat using cultivar mixtures. *Plant Pathology* **69**: 1655–1665.

Mikaberidze A, McDonald BA, Bonhoeffer S. **2015**. Developing smarter host mixtures to control plant disease. *Plant Pathology* **64**: 996–1004.

Morais D, Gélisse S, Laval V, Sache I, Suffert F. **2015**. Inferring the origin of primary inoculum of Zymoseptoria tritici from differential adaptation of resident and immigrant populations to wheat cultivars. *European Journal of Plant Pathology*.

Mundt CC. **2002**. Use of multiline cultivars and cultivar mixtures for disease management. *Annual Review of Phytopathology* **40**: 381–410.

Mundt C, Browning G. **1985**. Development of crown rust epidemics in genetically diverse oat populations: effect of genotype unit area. *Phytopathology* **75**: 607–610.

Mundt CC, Leonard KJ. **1986**. Effect of host genotype unit area on development of focal epidemics of bean rust and common maize rust in mixtures of resistant and susceptible plants. *Phytopathology* **76**: 895–900.

Mundt CC, Sackett KE, Wallace LD. **2011**. Landscape heterogeneity and disease spread: experimental approaches with a plant pathogen. *Ecological Applications* **21**: 321–328.

Newton AC, Begg GS, Swanston JS. **2009**. Deployment of diversity for enhanced crop function. *Annals of Applied Biology* **154**: 309–322.

Newton AC, Guy DC. **2009**. The effects of uneven, patchy cultivar mixtures on disease control and yield in winter barley. *Field Crops Research* **110**: 225–228.

Ntahimpera N, Ellis M, Wilson LL, Madden L. **1998**. Effects of a cover crop on splash dispersal of Colletotrichum acutatum conidia. *Phytopathology*.

Papaïx J, Adamczyk-Chauvat K, Bouvier A, Kiêu K, Touzeau S, Lannou C, Monod H. **2014**. Pathogen population dynamics in agricultural landscapes: the Ddal modelling framework. *Infection, Genetics and Evolution: Journal of Molecular Epidemiology and Evolutionary Genetics in Infectious Diseases* **27**: 509–520.

Pariaud B, Ravigné V, Halkett F, Goyeau H, Carlier J, Lannou C. **2009**. Aggressiveness and its role in the adaptation of plant pathogens. *Plant Pathology* **58**: 409–424.

Précigout P-A, Claessen D, Makowski D, Robert C. **2020a**. Does the latent period of leaf fungal pathogens reflect their trophic type? A meta-analysis of biotrophs, hemibiotrophs, and necrotrophs. *Phytopathology®* **110**: 345–361.

Précigout P-A, Claessen D, Robert C. **2017**. Crop fertilization impacts epidemics and optimal latent period of biotrophic fungal pathogens. *Phytopathology®* **107**: 1256–1267.

Précigout P-A, Robert C, Claessen D. **2020b**. Adaptation of biotrophic leaf pathogens to fertilization-mediated changes in plant traits: a comparison of the optimization principle to invasion fitness. *Phytopathology®* **110**: 1039–1048.

Ratnadass A, Fernandes P, Avelino J, Habib R. **2012**. Plant species diversity for sustainable management of crop pests and diseases in agroecosystems: a review. *Agronomy for Sustainable Development* **32**: 273–303.

Rimbaud L, Fabre F, Papaïx J, Moury B, Lannou C, Barrett LG, Thrall PH. **2021**. Models of plant resistance deployment. *Annual Review of Phytopathology* **59**: null.

Robert C, Bancal M-O, Lannou C. **2002**. Wheat leaf rust uredospore production and carbon and nitrogen export in relation to lesion size and density. *Phytopathology®* **92**: 762–768.

Robert C, Bancal M-O, Lannou C. **2004a**. Wheat Leaf Rust Uredospore Production on Adult Plants: Influence of Leaf Nitrogen Content and Septoria tritici Blotch. *Phytopathology®* **94**: 712–721.

Robert C, Bancal M-O, Ney B, Lannou C. **2005**. Wheat leaf photosynthesis loss due to leaf rust, with respect to lesion development and leaf nitrogen status. *New Phytologist* **165**: 227–241.

Robert C, Bancal M, Nicolas P, Lannou C, Ney B. **2004b**. Analysis and modelling of effects of leaf rust and Septoria tritici blotch on wheat growth. *Journal of Experimental Botany* **55**: 1079–1094.

Robert C, Fournier C, Andrieu B, Ney B. **2008**. Coupling a 3D virtual wheat (Triticum aestivum) plant model with a Septoria tritici epidemic model (Septo3D): a new approach to investigate plant-pathogen interactions linked to canopy architecture. *Functional plant biology: FPB* **35**: 997–1013.

Robert C, Garin G, Abichou M, Houlès V, Pradal C, Fournier C. **2018**. Plant architecture and foliar senescence impact the race between wheat growth and Zymoseptoria tritici epidemics. *Annals of Botany* **121**: 975–989.

Sache I, De Vallavieille-Pope C. **1993**. Comparison of the Wheat Brown and Yellow Rusts for Monocyclic Sporulation and Infection Processes, and their Polycyclic Consequences. *Journal of Phytopathology* **138**: 55–65.

Sache I, Zadoks JC. **1996**. Spread of faba bean rust over a discontinuous field. *European Journal of Plant Pathology* **102**: 51–60.

Saint-Jean S, Chelle M, Huber L. **2004**. Modelling water transfer by rain-splash in a 3D canopy using Monte Carlo integration. *Agricultural and Forest Meteorology* **121**: 183–196.

Sanner J, Classens D, Robert C, Levionnois S, Pradal C, Fournier C. **2022**. *openalea/EpyMix: EpyMix version 1.0*. Zenodo.

Sapoukhina N, Paillard S, Dedryver F, de Vallavieille-Pope C. **2013**. Quantitative plant resistance in cultivar mixtures: wheat yellow rust as a modeling case study. *New Phytologist* **200**: 888–897.

Schoeny A, Menat J, Darsonval A, Rouault F, Jumel S, Tivoli B. **2008**. Effect of pea canopy architecture on splash dispersal of Mycosphaerella pinodes conidia. *Plant Pathology* **57**: 1073–1085.

Suffert F, Sache I. **2011**. Relative importance of different types of inoculum to the establishment of [i]Mycosphaerella graminicola[/i] in wheat crops in north-west Europe. *Plant Pathology* **60**: 878.

880 **Suffert F, Sache I, Lannou C**. **2011**. Early stages of septoria tritici blotch epidemics of winter wheat:
881 build-up, overseasoning, and release of primary inoculum. *Plant Pathology* **60**: 166–177.

882 **Suffert F, Sache I, Lannou C**. **2013**. Assessment of quantitative traits of aggressiveness in
883 Mycosphaerella graminicola on adult wheat plants. *Plant Pathology* **62**: 1330–1341.

884 **de Vallavieille-Pope C, Ali S, Leconte M, Enjalbert J, Delos M, Rouzet J**. **2012**. Virulence dynamics
885 and regional structuring of Puccinia striiformis f. sp. tritici in France Between 1984 and 2009. *Plant*
886 *Disease* **96**: 131–140.

887 **Větrovský T, Kohout P, Kopecký M, Machac A, Man M, Bahnmann BD, Brabcová V, Choi J,**
888 **Meszárošová L, Human ZR, *et al.* 2019**. A meta-analysis of global fungal distribution reveals climate-
889 driven patterns. *Nature Communications* **10**: 5142.

890 **Vidal T, Boixel A-L, Durand B, Vallavieille-Pope C de, Huber L, Saint-Jean S**. **2017a**. Reduction of
891 fungal disease spread in cultivar mixtures: Impact of canopy architecture on rain-splash dispersal and
892 on crop microclimate. *Agricultural and Forest Meteorology* **246**: 154.

893 **Vidal T, Gigot C, de Vallavieille-Pope C, Huber L, Saint-Jean S**. **2018**. Contrasting plant height can
894 improve the control of rain-borne diseases in wheat cultivar mixture: modelling splash dispersal in 3-
895 D canopies. *Annals of Botany* **121**: 1299–1308.

896 **Vidal T, Lusley P, Leconte M, Vallavieille-Pope C de, Huber L, Saint-Jean S**. **2017b**. Cultivar
897 architecture modulates spore dispersal by rain splash: A new perspective to reduce disease
898 progression in cultivar mixtures. *PLOS ONE* **12**: e0187788.

899 **Wallace JS**. **1997**. Evaporation and radiation interception by neighbouring plants. *Quarterly Journal of*
900 *the Royal Meteorological Society* **123**: 1885–1905.

901 **Wolfe MS**. **1985**. The current status and prospects of multiline cultivars and variety mixtures for
902 disease resistance. *Annual Review of Phytopathology* **23**: 251–273.

903 **Zawolek MW, Zadoks JC**. **1992**. Studies in focus development: an optimum for the dual dispersal of
904 plant pathogens. *Phytopathology*.

905

906 **TABLES**

907 **Table 1**. List of parameters

908
909

910

Symbol	Standard value		Unit	Designation	Reference	
			General parameters			
t_{start}	0		dd	Start date of the cropping season	-	-
t_{end}	2500		dd	End date of the cropping season	Précigout et al. (2017)	
			Wheat and companion growth parameters			
μ	0.0025		-	Crop mortality rate	(Dornbusch *et al.*, 2011; Baccar, 2011)	
β	0.009		-	Crop growth rate parameter	(Dornbusch *et al.*, 2011; Baccar, 2011)	
t_{onto}	1400		dd	Start of senescence	(Dornbusch *et al.*, 2011; Baccar, 2011)	
K	4.8		-m^2 m^{-2}	Carrying capacity	(Dornbusch *et al.*, 2011; Baccar, 2011)	
h	1		-	Dominance factor	-	-
b	1		-	Beer-Lambert-like parameter of spore interception rate by crop canopy used as a proxy for canopy porosity	-	-
			Epidemic parameters			
	WLR	STB			WLR	STB
t_{inf}	800-1200	0	dd	Start date of the epidemic	Duvivier et al. (2016)	Suffert and Sache (2011)
t_{out}		700	dd	Date at which leaves are no longer reachable by soil spores (for STB only)	-	Suffert et al. (2011)
λ	100	200	dd	Latent period	Robert et al. (2004a)	(Robert *et al.*, 2004b))
δ_{EI}	50	50	dd	Variability parameter for the latent period	(Précigout *et al.*, 2020a))	
σ	U*: 1,500,000	P*: 40,000,000 A*: 0.2 * P	-	Spore production rate per unit of infected LAI	(Sache & De Vallavieille-Pope, 1993) and consistency test	(Suffert *et al.*, 2013) and consistency test
ψ		0.3	-	Emptying rates of pycnids during a rain event (for STB only)		(Eyal, 1971)
s_0	0.0001	0.0001	m^2	Lesion size on crop canopy	(Robert *et al.*, 2004a))	(Robert *et al.*, 2008)
π_{inf}	0.0002	0.0002	-	Infection probability	Consistency test	
ρ	0.0015	0.0002	-	Spore mortality rate in pool P	Consistency test and Précigout et al. (2017)	
θ	0.01	0.15	-	Spore survival rate during intercropping season	Consistency test and Précigout et al. (2017)	

$Sp_{,ext}$	2,000	20,000	-	Number of spores coming from the landscape into the canopy every 20 dd	(Duvivier *et al.*, 2016)) and consistency test	(Suffert & Sache, 2011) and consistency test
Sp_{init}	350,000	10,000,000			-	-

*U: urediospores, dispersed by wind; P: pycnidiospores, dispersed by wind; A: ascospores, dispersed by rain splash

911

912 **Table 2**. List of model state variables

Symbol	Unit	Designation
LAI	$m^2\ m^{-2}$	Leaf area index of the canopy
S	$m^2\ m^{-2}$	Susceptible healthy LAI of the canopy
E	$m^2\ m^{-2}$	Exposed and infected LAI of the canopy
I	$m^2\ m^{-2}$	Infectious LAI of the canopy
R	$m^2\ m^{-2}$	Removed and senesced LAI of the canopy
c	-	Canopy growth rate
η	-	Vector for age of infection, from E to I state
P	-	Number of spores in the soil reservoir
Sp_{soil}	-	Number of spores remobilized from P that potentially infect the canopy
Sp_{ext}	-	Number of spores from outside the canopy that potentially infect the canopy
Sp_{canopy}	-	Number of spores produced by and potentially infecting the canopy
N_{sp}	-	Total number of spores potentially infecting the canopy
ε	-	Fraction of spores intercepted by the canopy
N_g	-	Number of spores germinating after interception by the canopy
F_{cont}	-	Canopy fraction intercepting the spores that potentially lead to lesions
S_i	-	Quantity of S tissues becoming infected
I_{vid}	$m^2\ m^{-2}$	Cumulated canopy surface that passes through the infectious state I
$AUDPC$	-	Area under the disease progress curve (I)

913

914

915

916 **FIGURE LEGENDS**
917

918 **Fig. 1.** Conceptual map of the model system. *S*: susceptible; *E*: exposed (latent); *I*: infectious;
919 *R*: removed. N_{sp}: total number of spores dispersed; Sp_{ext}: number of spores from outside the
920 system; Sp_{soil}: number of spores from the soil; Sp_{canopy}: number of spores produced by lesions.
921 See Table 1 for parameter abbreviations.
922

923 **Fig. 2.** Variation of theoretical wheat leaf area index (LAI; dashed black curves), susceptible
924 LAI (green curves), cumulated infectious LAI (orange curves), and senescent LAI (black
925 curves) over three cropping seasons for two wheat diseases in favorable weather conditions. **A**,
926 Pure wheat for WLR. **B**, equi-proportional mixture for wheat leaf rust (WLR). **C**, Pure wheat
927 for Septoria tritici blotch (STB). **D**, equi-proportional mixture for STB. For mixtures, the
928 growth curve of the companion species is equivalent to that of the theoretical wheat LAI. For
929 STB, the differences between crop seasons are also driven by different weather conditions.
930

931 **Fig. 3.** Local sensitivity analyses of wheat disease intensity in favorable weather conditions to
932 all model parameters for wheat leaf rust (WLR) (**A**) and Septoria tritici blotch (STB) (**B**). For
933 each figure, only the top ten parameters (highest absolute values of relative sensibility) are
934 shown. White bars indicate that increasing the parameter will increase the infection rate,
935 whereas black bars indicate that decreasing the parameter will increase the infection rate. The
936 last subscript, when present, indicates whether the change refers to wheat ("W"), companion
937 species ("C"), WLR uredospores ("U"), STB pycnidiospores ("P"), or STB ascospores ("A").
938 The complete list of abbreviations is shown in Table 1.
939

940 **Fig. 4.** Global sensitivity analysis of the relative area under disease progress curve (*AUDPC*)
941 to the companion proportion for wheat leaf rust (WLR) in favorable weather conditions for
942 different companion parameters. **A**, Dominance factor (h). **B**, Beer-Lambert of interception
943 (*ber*). **C**, Growth rate (β). **D**, Mortality rate (μ). **E**, Start of senescence (t_{onto}). **F**, Relative sowing
944 date (*delta*). Black line: standard parameter value. Two-dashed and dotted lines: 50% and -50%
945 variation of the parameter, respectively.
946

947 **Fig. 5.** Global sensitivity analysis of the relative area under disease progress curve (*AUDPC*)
948 to the variation of companion parameters, for wheat leaf rust (WLR) in favorable weather
949 conditions. **A**, Dominance factor (h). **B**, Beer-Lambert of interception (*ber*). **C**, Growth rate (β).

D, Mortality rate (μ). **E**, Senescence earliness (t_{onto}). **F**, Relative sowing date (*delta*). The larger the dashed line, the greater the proportion of wheat in the mixture: 0.1, 0.3, 0.5, 0.7, 0.9.

Fig. 6. Decomposition of the dilution and barrier effects for the protective effect of mixtures according to the wheat proportion in the mixture, in favorable weather conditions. **A**, Protective effect according to the companion proportion for wheat leaf rust (WLR). **B**, Protective effect according to the companion proportion for Septoria tritici blotch (STB). Blue: dilution effect (i.e., pure susceptible crop only); orange: protective effect due to the barrier effect; black: total mixture effect.

959 **SUPPLEMENTARY INFORMATION**

960 **Fig. S1.** Variation of theoretical wheat leaf are index (LAI; dashed black curve) and cumulated
961 infectious LAI (filled black curve) over three cropping seasons for two wheat diseases in
962 favorable weather conditions. Sensitivity of cumulated infectious LAI (colored dashed lines) to
963 each of the six parameters (σ: orange, π_{inf}: yellow, ρ: light blue, θ: green, $Sp_{,ext}$: pink, Sp_{init}: dark
964 blue) is tested independently, at -10% and +10% of parameter values. **A**, Pure wheat for WLR.
965 **B**, equi-proportional mixture for wheat leaf rust (WLR). **C**, Pure wheat for Septoria tritici blotch
966 (STB). **D**, equi-proportional mixture for STB. For mixtures, the growth curve of the companion
967 species is equivalent to the theoretical wheat LAI. For STB, the differences between crop
968 seasons are also driven by different weather conditions.
969
970 **Fig. S2.** Growth curves of the companion species while varying the growth rate β (**A**), mortality
971 rate μ (**B**), start of senescence t_{onto} (**C**), and relative sowing date *delta* (D) parameters by -30%
972 (dashed) and +30% (dotted), respectively. Black: the growth curve for standard parameters for
973 wheat and companion.
974
975 **Fig. S3.** Global sensitivity analysis of the relative area under disease progress curve (*AUDPC*)
976 to companion proportion for Septoria tritici blotch (STB) in favorable weather conditions for
977 different companion parameters. **A**, Dominance factor (*h*). **B**, Beer-Lambert of interception
978 (*ber*). **C**, Growth rate (β). **D**, Mortality rate (μ). **E**, Start of senescence (t_{onto}). **F**, Relative sowing
979 date (*delta*). Two-dashed and dotted lines correspond to 50% and -50% variation of the
980 parameter, respectively.
981
982 **Fig. S4.** Global sensitivity analysis of the relative area under disease progress curve (*AUDPC*)
983 to the variation of companion parameters for Septoria tritici blotch (STB) in favorable weather
984 conditions. **A**, Dominance factor (*h*). **B**, Beer-Lambert of interception (*ber*). **C**, Growth rate (β).
985 **D**, Mortality rate (μ). **E**, Start of senescence (t_{onto}). **F**, Relative sowing date (*delta*). The larger
986 the dashed line, the greater the proportion of wheat in the mixture: 0.1, 0.3, 0.5, 0.7, 0.9.
987
988 **Fig. S5.** Global sensitivity analysis of the relative area under disease progress curve (*AUDPC*)
989 to companion proportion and for different weather conditions. **A**, Rust, black: favorable
990 conditions (t_{inf} = 80 dd; standard parameter value in Fig. 3 and Fig. 5), blue: unfavorable
991 conditions (t_{inf} = 120 dd), orange: average conditions (t_{inf} = 100 dd). **B**, Septoria, black: average
992 conditions (average rainfall in 1997; standard parameter value in Fig. 4 and 6), blue:

993 unfavorable conditions (low rainfall in 1995), orange: favorable conditions (high rainfall in
994 2000).
995
996 **Fig. S6.** Global sensitivity analysis of the relative area under disease progress curve (*AUDPC*)
997 to variation of companion parameters for wheat leaf rust (WLR) in different weather conditions.
998 **A**, Dominance factor (*h*). **B**, Beer-Lambert of interception (*ber*). **C**, Growth rate (β). **D**,
999 Mortality rate (μ). **E**, Start of senescence (t_{onto}). **F**, Relative sowing date (*delta*). The larger the
1000 dashed line, the greater the proportion of wheat in the mixture: 0.1, 0.5, 0.9. Black: favorable
1001 conditions (t_{inf} = 80 dd; standard parameter value in Fig. 3 and Fig. 5); blue: unfavorable
1002 conditions (t_{inf} = 120 dd); orange: average conditions (t_{inf} = 100 dd).
1003
1004 **Fig. S7.** Global sensitivity analysis of the relative area under disease progress curve (*AUDPC*)
1005 to variation of companion parameters for Septoria tritici blotch (STB) in different weather
1006 conditions. **A**, Dominance factor (*h*). **B**, Beer-Lambert of interception (*ber*). **C**, Growth rate (β).
1007 **D**, Mortality rate (μ). **E**, Start of senescence (t_{onto}). **F**, Relative sowing date (*delta*). The larger
1008 the dashed line, the greater the proportion of wheat in the mixture: 0.1, 0.5, 0.9. Black: average
1009 conditions (average rainfall in 1997; standard parameter value in Fig. 4 and 6); blue:
1010 unfavorable conditions (low rainfall in 1995); orange: favorable conditions (low rainfall in
1011 2000).

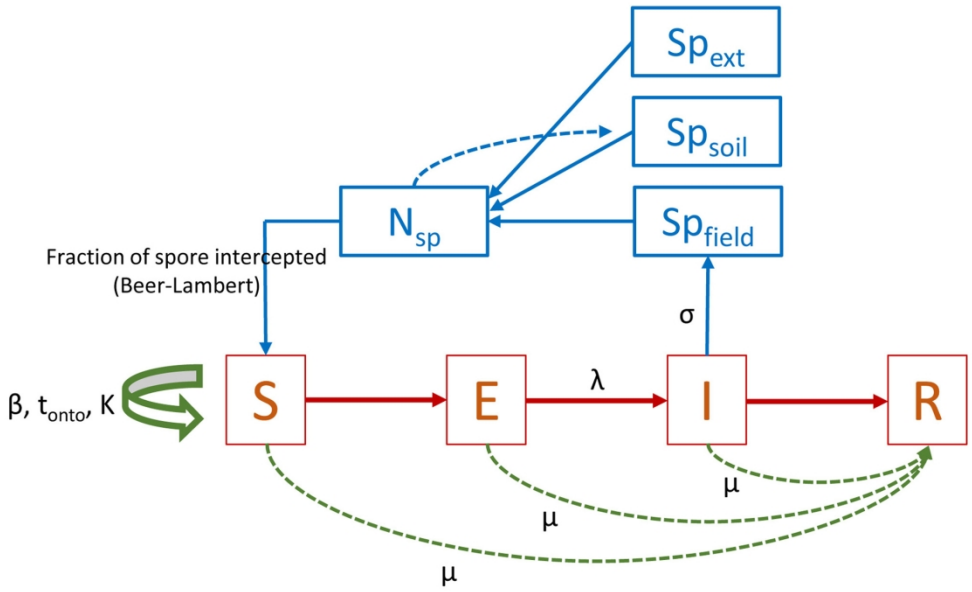

Fig. 1. Conceptual map of the model system. S: susceptible; E: exposed (latent); I: infectious; R: removed. Nsp: total number of spores dispersed; Spext: number of spores from outside the system; Spsoil: number of spores from the soil; Spcanopy: number of spores produced by lesions. See Table 1 for parameter abbreviations.

177x108mm (300 x 300 DPI)

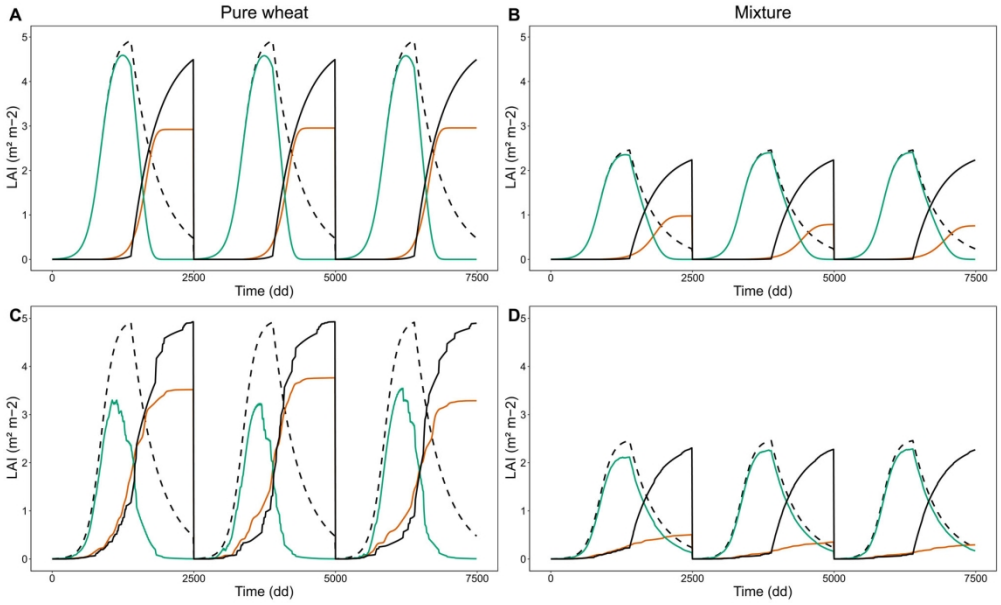

Fig. 2. Variation of theoretical wheat leaf area index (LAI; dashed black curves), susceptible LAI (green curves), cumulated infectious LAI (orange curves), and senescent LAI (black curves) over three cropping seasons for two wheat diseases in favorable weather conditions. A, Pure wheat for WLR. B, equi-proportional mixture for wheat leaf rust (WLR). C, Pure wheat for Septoria tritici blotch (STB). D, equi-proportional mixture for STB. For mixtures, the growth curve of the companion species is equivalent to that of the theoretical wheat LAI. For STB, the differences between crop seasons are also driven by different weather conditions.

171x102mm (300 x 300 DPI)

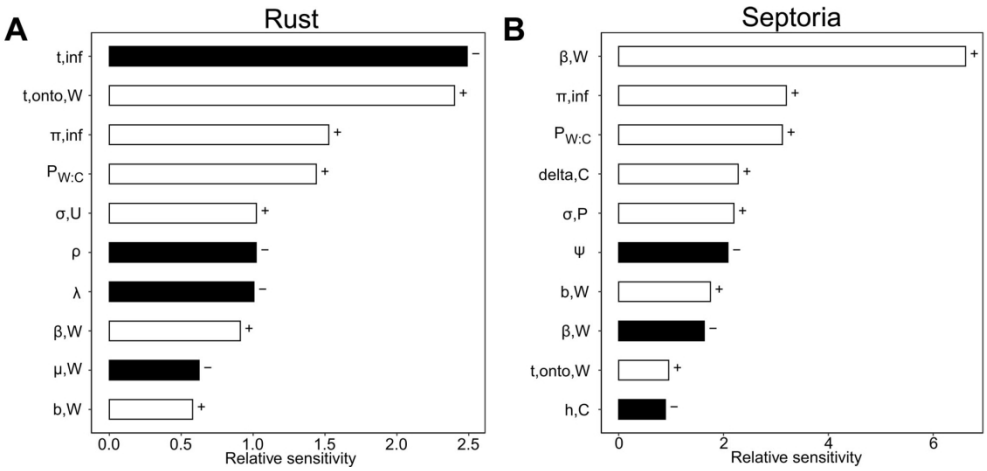

Fig. 3. Local sensitivity analyses of wheat disease intensity in favorable weather conditions to all model parameters for wheat leaf rust (WLR) (A) and Septoria tritici blotch (STB) (B). For each figure, only the top ten parameters (highest absolute values of relative sensibility) are shown. White bars indicate that increasing the parameter will increase the infection rate, whereas black bars indicate that decreasing the parameter will increase the infection rate. The last subscript, when present, indicates whether the change refers to wheat ("W"), companion species ("C"), WLR uredospores ("U"), STB pycnidiospores ("P"), or STB ascospores ("A"). The complete list of abbreviations is shown in Table 1.

171x79mm (300 x 300 DPI)

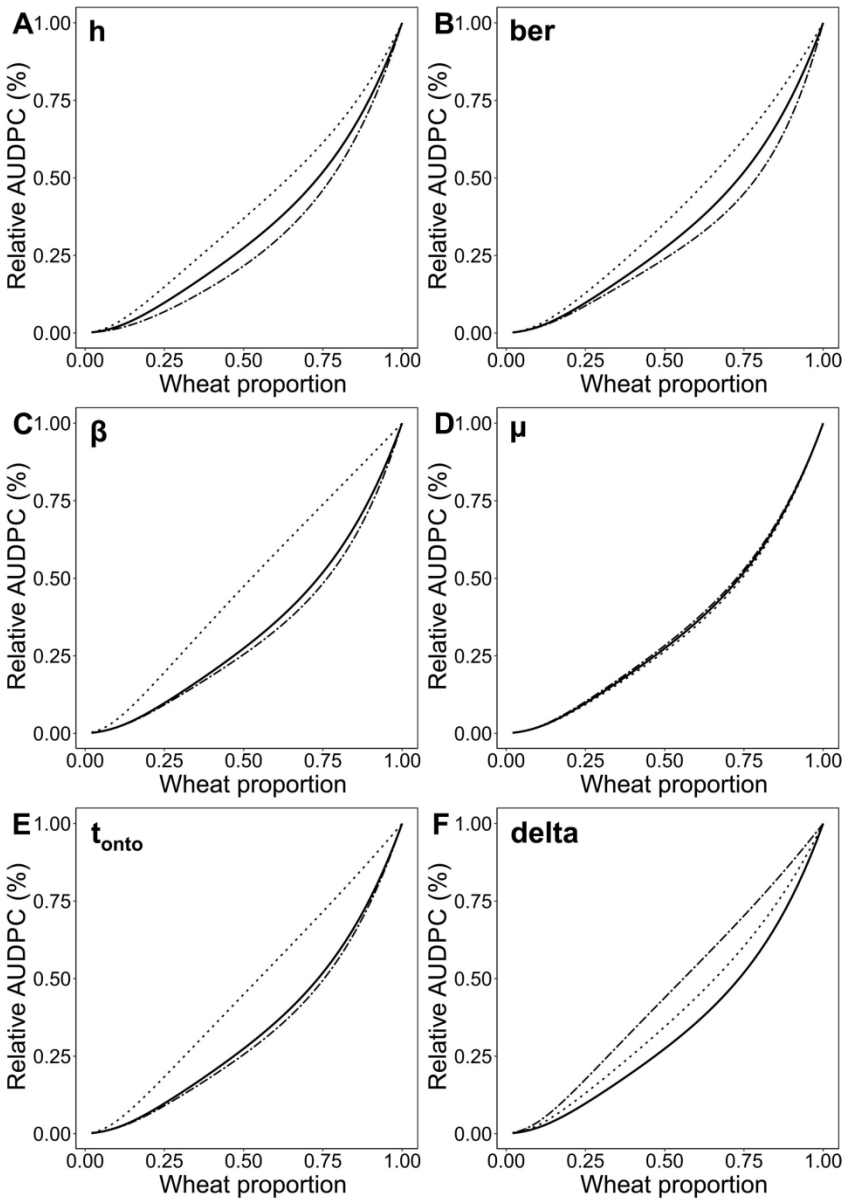

Fig. 4. Global sensitivity analysis of the relative area under disease progress curve (AUDPC) to the companion proportion for wheat leaf rust (WLR) in favorable weather conditions for different companion parameters. A, Dominance factor (h). B, Beer-Lambert of interception (ber). C, Growth rate (β). D, Mortality rate (μ). E, Start of senescence (tonto). F, Relative sowing date (delta). Black line: standard parameter value. Two-dashed and dotted lines: 50% and -50% variation of the parameter, respectively.

171x243mm (300 x 300 DPI)

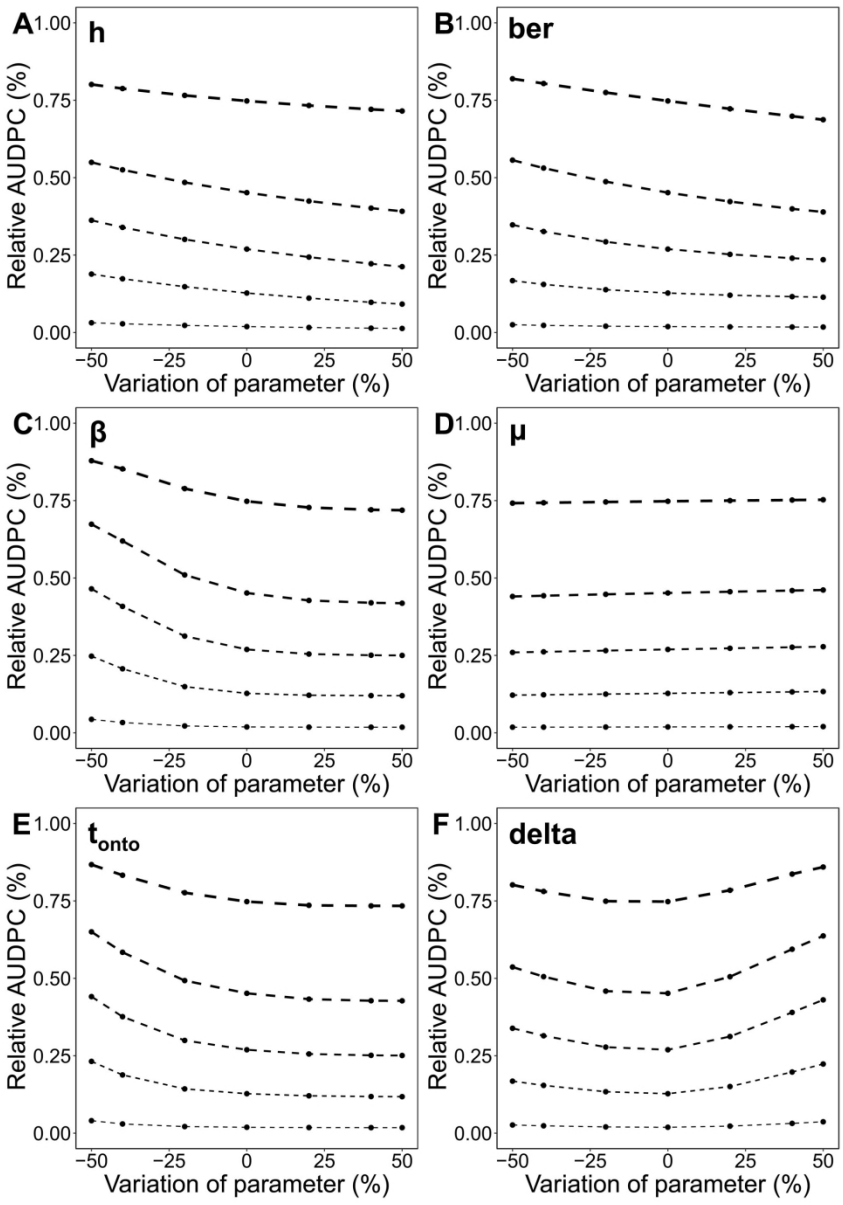

Fig. 5. Global sensitivity analysis of the relative area under disease progress curve (AUDPC) to the variation of companion parameters, for wheat leaf rust (WLR) in favorable weather conditions. A, Dominance factor (h). B, Beer-Lambert of interception (ber). C, Growth rate (β). D, Mortality rate (μ). E, Senescence earliness (tonto). F, Relative sowing date (delta). The larger the dashed line, the greater the proportion of wheat in the mixture: 0.1, 0.3, 0.5, 0.7, 0.9.

171x243mm (300 x 300 DPI)

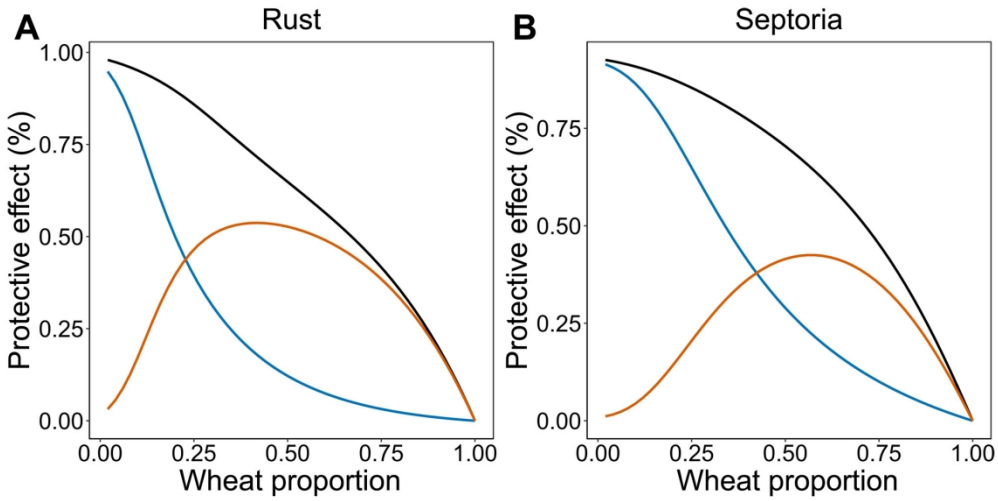

Fig. 6. Decomposition of the dilution and barrier effects for the protective effect of mixtures according to the wheat proportion in the mixture, in favorable weather conditions. A, Protective effect according to the companion proportion for wheat leaf rust (WLR). B, Protective effect according to the companion proportion for Septoria tritici blotch (STB). Blue: dilution effect (i.e., pure susceptible crop only); orange: protective effect due to the barrier effect; black: total mixture effect.

171x85mm (300 x 300 DPI)

Supplemental method S1: Parameterization of growth curves

The wheat growth model was parameterized and calibrated based on dynamic data relating to the leaf area index (LAI) for winter wheat from Baccar et al. (Baccar 2011; Dornbusch et al. 2011).

Experimental design, treatment, and measurement

The experiment was conducted in the INRA experimental fields in Thiverval-Grignon, France (48°51'N, 1°58'E) on silty loam soil. *T. aestivum* Cv. 'Soissons' was grown in 2008/2009 and sowed in mid-November. Three treatments were prepared corresponding to three different sowing densities: 77, 228, and 514 plants m^{-2} referred to as low density (D1), intermediate density (D2), and high density (D3), respectively. Each treatment was carried out in three parallel plots, at least 30 m in length and spaced 0.2 m apart. Each plot consisted of nine rows of plants with an interrow distance of e = 0.175 m. The space between plots was used as an access path, so the two external rows on each side of the plots were considered as borders and not used for measurements.

LAI was measured for each treatment with three repetitions. For each repetition, five LAI measurements were made at five sampling dates after sowing: 353, 627, 911, 1187, and 1559 dd. LAI was measured on a subplot of 0.35 m². At the subplot level, LAI was determined by (i) measuring the LAI and dry mass of five plants, (ii) measuring the dry mass of the wheat in the entire subplot, and (iii) estimating LAI at the whole subplot level. More details are provided in Baccar (2011) and Dornbusch et al. (2011).

Parameterization and calibration

The numerical solution of the logistic growth model for wheat presented in the main Materials and Methods section was fitted to the LAI observations, for the three density treatments (Fig. S8). For each treatment, we used the mean of the three repetitions for each sampling date. Two parameters were changed to best fit the experimental data in the increasing part of the curve: β_W, and K. For this nonlinear regression analysis, we used the Nelder-Mead algorithm (Nelder and Mead 1965) within the `optim` function in the programming language R (R Core Team 2018). The decreasing part of the curve was fitted manually relying on a function of distance minimization and by changing the parameter μ_W. Parameter values for each density treatment are presented in Table S1.

In our study, we took as reference parameter values those relating to the density treatment D3 (514 plants m^{-2}). This was motivated by the fact that the large LAI and sowing density better reflect the intercropping context.

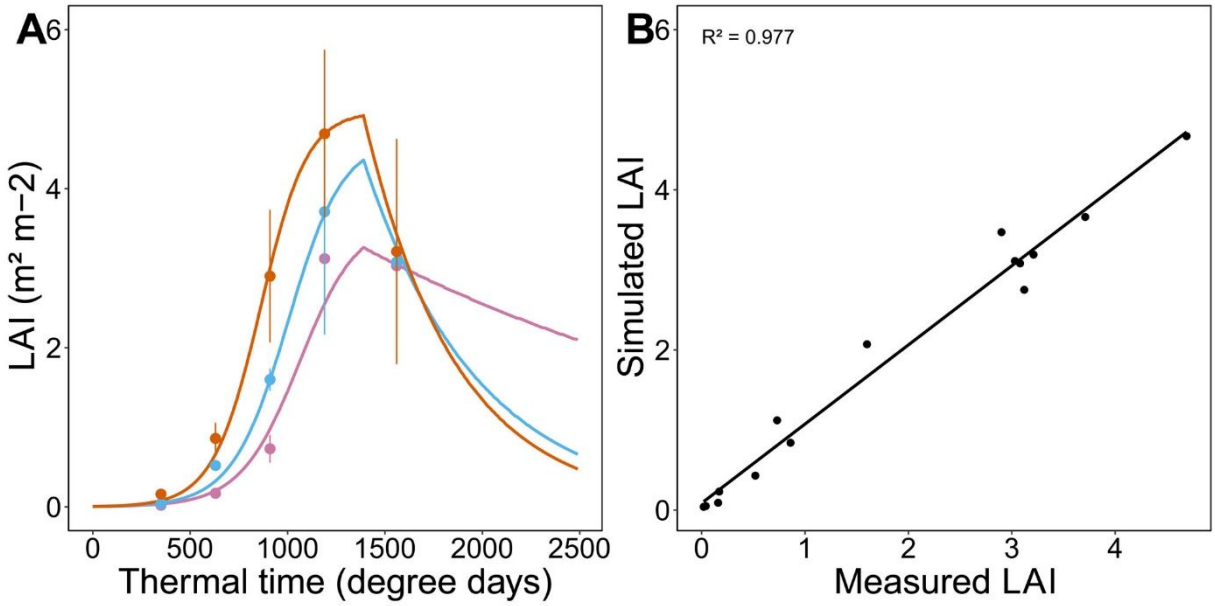

Fig. S8. Calibration of the logistic growth model to leaf area index (LAI) data. **A**, Model fitting to the LAI data. Blue: D1; pink: D2; orange: D3; black: mean of the three treatments. **B**, Simulated LAI versus measured LAI across the three treatments.

Table S1. Parameter values of the logistic growth model for the three density treatments.

	Parameters		
Treatment	**β**	**μ**	**K**
D1	0.067	0.004	3.6
D2	0.071	0.017	4.62
D3	0.083	0.021	4.97

LITERATURE CITED

Baccar, R. 2011. Plasticité de l'architecture du blé d'hiver modulée par la densité et la date de semis et son effet sur les épidémies de Septoria tritici. Available at: https://www.theses.fr/2011AGPT0031 [Accessed February 7, 2023].

Dornbusch, T., Baccar, R., Watt, J., Hillier, J., Bertheloot, J., Fournier, C., et al. 2011. Plasticity of winter wheat modulated by sowing date, plant population density and nitrogen fertilisation: Dimensions and size of leaf blades, sheaths and internodes in relation to their position on a stem. Field Crops Research. 121:116–124.

53 Nelder, J. A., and Mead, R. 1965. A Simplex Method for Function Minimization. The
54 Computer Journal. 7:308–313.

55 R Core Team. 2018. R: a language and environment for statistical computing. Available at:
56 https://www.gbif.org/fr/tool/81287/r-a-language-and-environment-for-statistical-computing
57 [Accessed February 15, 2021].

58

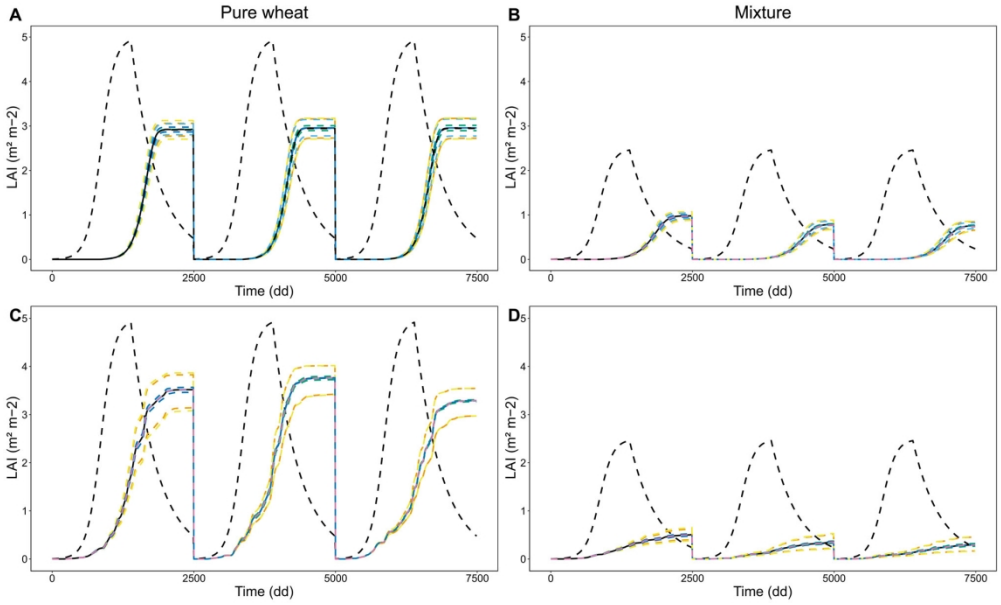

Fig. S1. Variation of theoretical wheat leaf are index (LAI; dashed black curve) and cumulated infectious LAI (filled black curve) over three cropping seasons for two wheat diseases in favorable weather conditions. Sensitivity of cumulated infectious LAI (colored dashed lines) to each of the six parameters (σ: orange, ninf: yellow, ρ: light blue, θ: green, Sp,ext: pink, Spinit: dark blue) is tested independently, at -10% and +10% of parameter values. A, Pure wheat for WLR. B, equi-proportional mixture for wheat leaf rust (WLR). C, Pure wheat for Septoria tritici blotch (STB). D, equi-proportional mixture for STB. For mixtures, the growth curve of the companion species is equivalent to the theoretical wheat LAI. For STB, the differences between crop seasons are also driven by different weather conditions.

171x102mm (300 x 300 DPI)

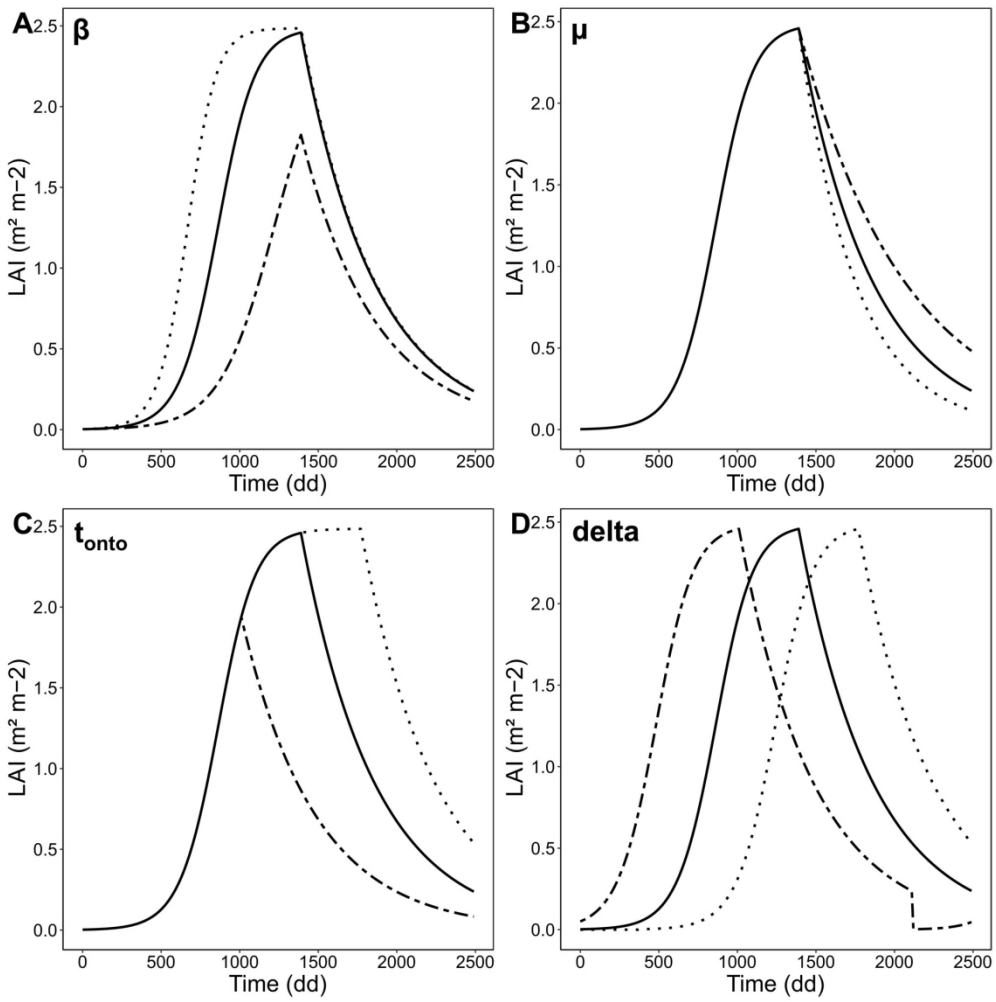

Fig. S2. Growth curves of the companion species while varying the growth rate β (A), mortality rate μ (B), start of senescence tonto (C), and relative sowing date delta (D) parameters by -30% (dashed) and +30% (dotted), respectively. Black: the growth curve for standard parameters for wheat and companion.

171x171mm (300 x 300 DPI)

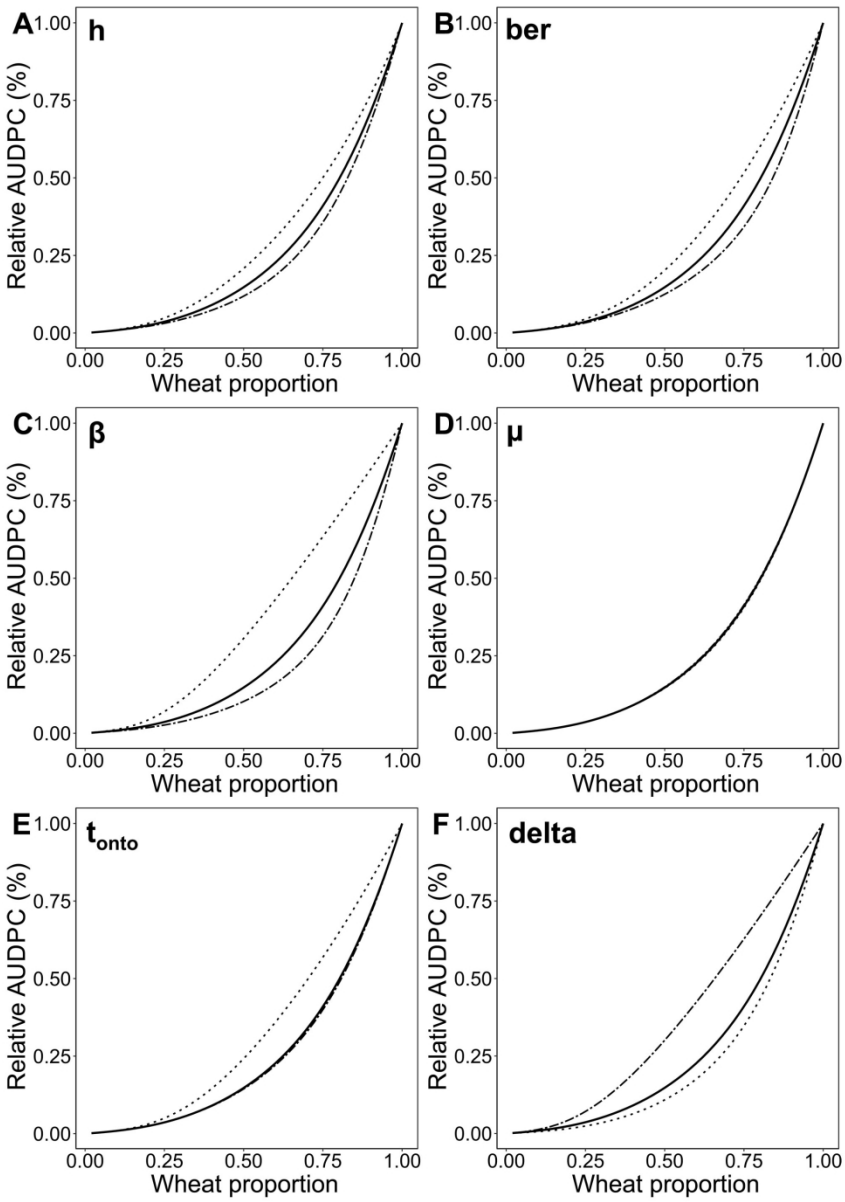

Fig. S3. Global sensitivity analysis of the relative area under disease progress curve (AUDPC) to companion proportion for Septoria tritici blotch (STB) in favorable weather conditions for different companion parameters. A, Dominance factor (h). B, Beer-Lambert of interception (ber). C, Growth rate (β). D, Mortality rate (μ). E, Start of senescence (tonto). F, Relative sowing date (delta). Two-dashed and dotted lines correspond to 50% and -50% variation of the parameter, respectively.

171x243mm (300 x 300 DPI)

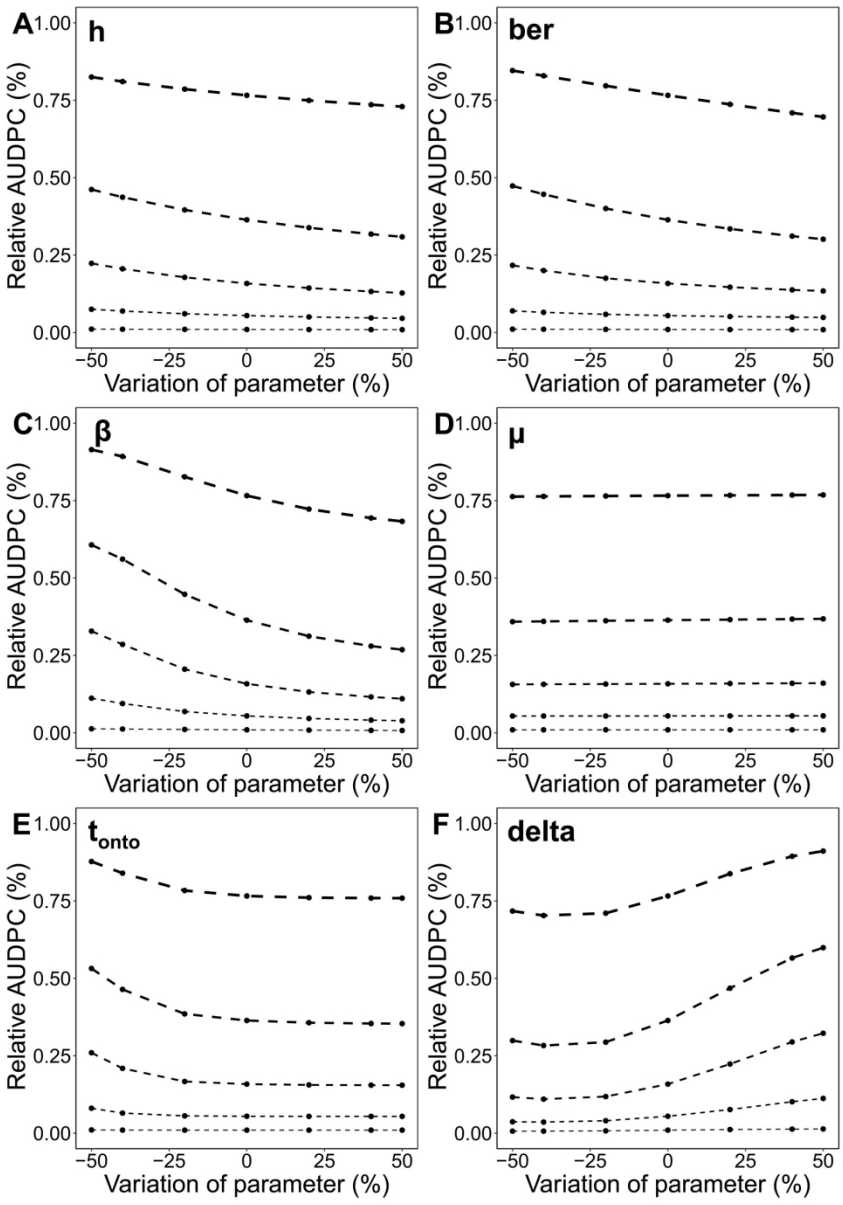

Fig. S4. Global sensitivity analysis of the relative area under disease progress curve (AUDPC) to the variation of companion parameters for Septoria tritici blotch (STB) in favorable weather conditions. A, Dominance factor (h). B, Beer-Lambert of interception (ber). C, Growth rate (β). D, Mortality rate (μ). E, Start of senescence (tonto). F, Relative sowing date (delta). The larger the dashed line, the greater the proportion of wheat in the mixture: 0.1, 0.3, 0.5, 0.7, 0.9.

171x243mm (300 x 300 DPI)

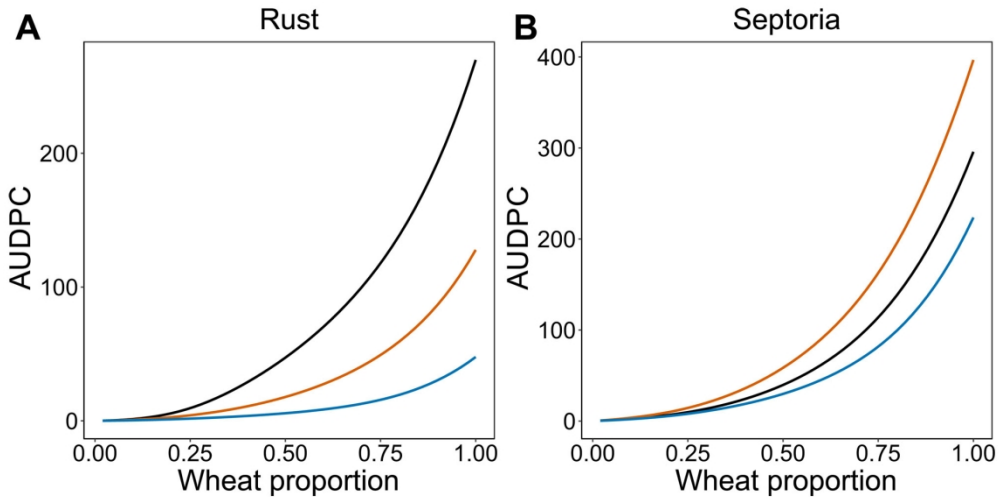

Fig. S5. Global sensitivity analysis of the relative area under disease progress curve (AUDPC) to companion proportion and for different weather conditions. A, Rust, black: favorable conditions (tinf = 80 dd; standard parameter value in Fig. 3 and Fig. 5), blue: unfavorable conditions (tinf = 120 dd), orange: average conditions (tinf = 100 dd). B, Septoria, black: average conditions (average rainfall in 1997; standard parameter value in Fig. 4 and 6), blue: unfavorable conditions (low rainfall in 1995), orange: favorable conditions (high rainfall in 2000).

171x85mm (300 x 300 DPI)

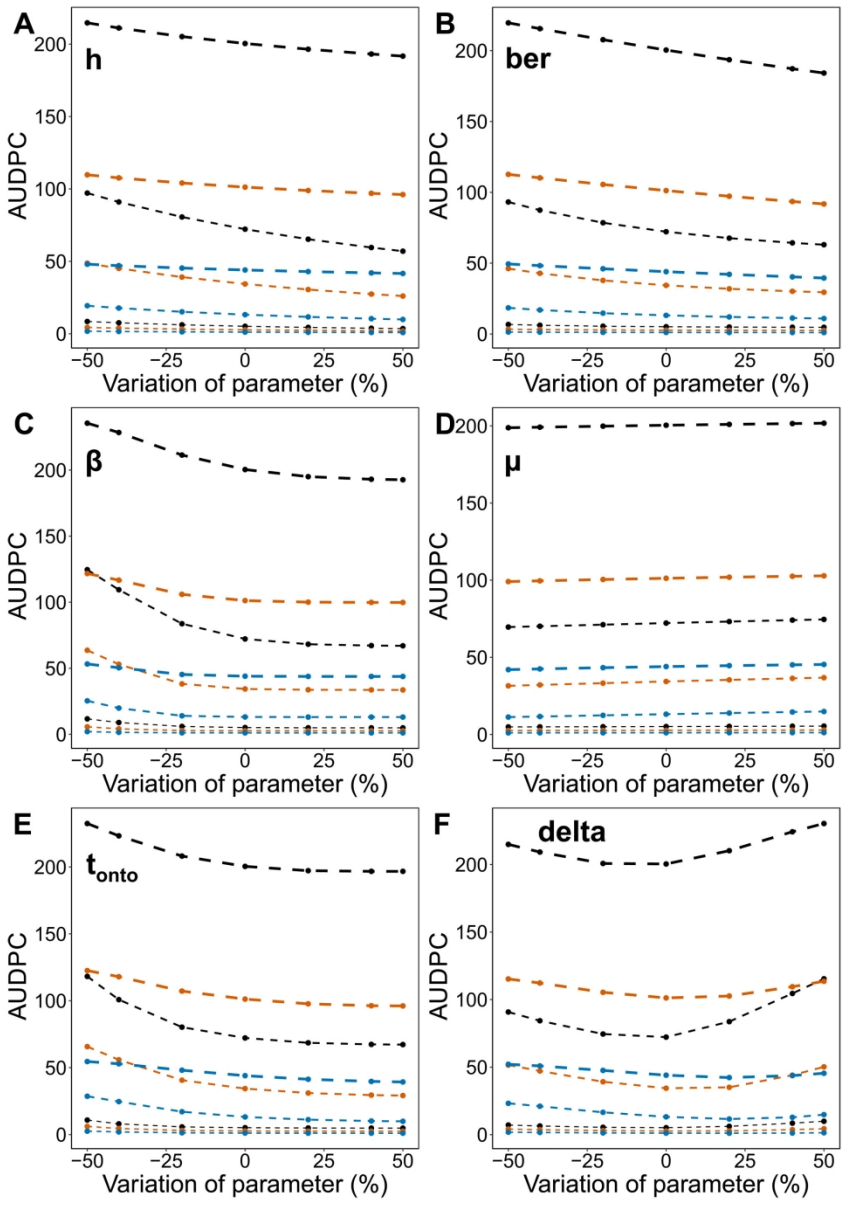

Fig. S6. Global sensitivity analysis of the relative area under disease progress curve (AUDPC) to variation of companion parameters for wheat leaf rust (WLR) in different weather conditions. A, Dominance factor (h). B, Beer-Lambert of interception (ber). C, Growth rate (β). D, Mortality rate (μ). E, Start of senescence (tonto). F, Relative sowing date (delta). The larger the dashed line, the greater the proportion of wheat in the mixture: 0.1, 0.5, 0.9. Black: favorable conditions (tinf = 80 dd; standard parameter value in Fig. 3 and Fig. 5); blue: unfavorable conditions (tinf = 120 dd); orange: average conditions (tinf = 100 dd).

171x243mm (300 x 300 DPI)

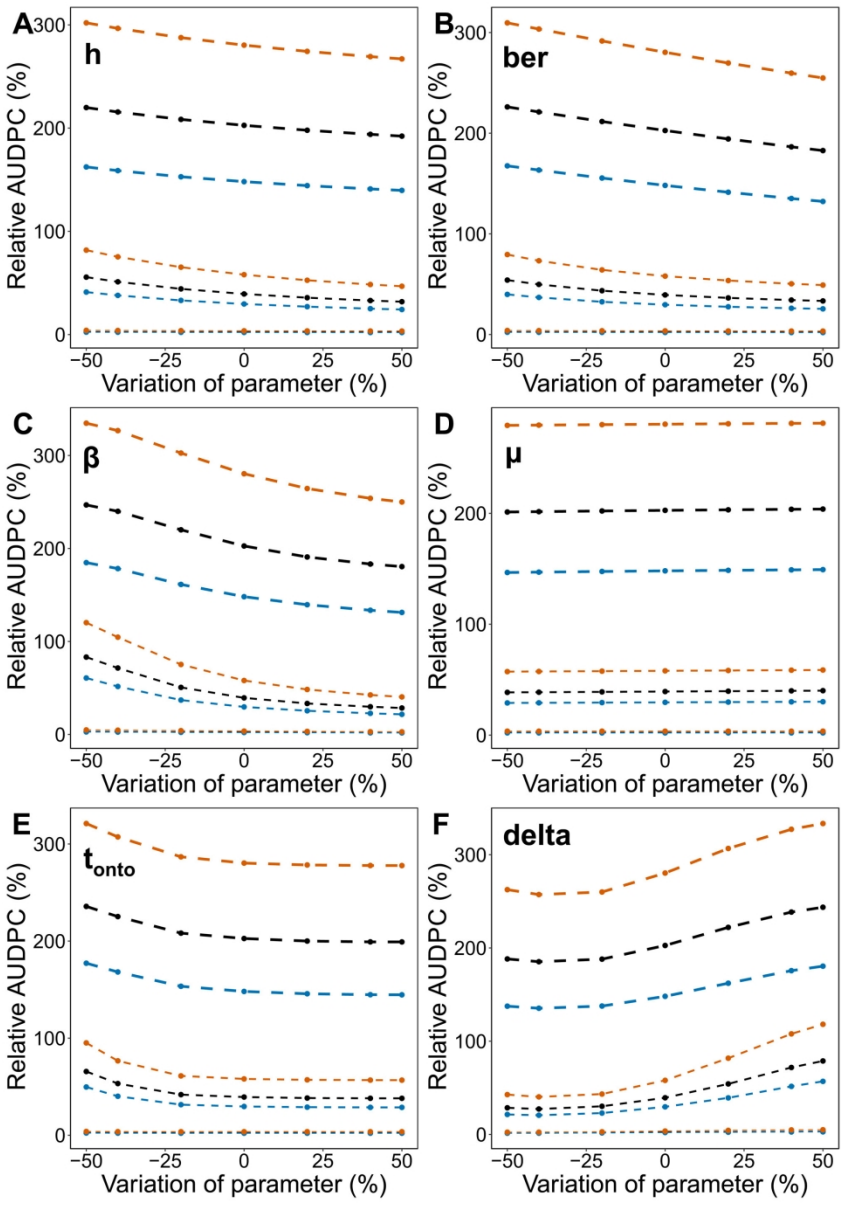

Fig. S7. Global sensitivity analysis of the relative area under disease progress curve (AUDPC) to variation of companion parameters for Septoria tritici blotch (STB) in different weather conditions. A, Dominance factor (h). B, Beer-Lambert of interception (ber). C, Growth rate (β). D, Mortality rate (μ). E, Start of senescence (tonto). F, Relative sowing date (delta). The larger the dashed line, the greater the proportion of wheat in the mixture: 0.1, 0.5, 0.9. Black: average conditions (average rainfall in 1997; standard parameter value in Fig. 4 and 6); blue: unfavorable conditions (low rainfall in 1995); orange: favorable conditions (low rainfall in 2000).

171x243mm (300 x 300 DPI)